Measurements of Industrial Fugitive Emissions by the FTIR Tracer Method (FTM)

Johan Mellqvist, Bill Arlander,
Bo Galle and Björn Bergqvist

Göteborg, January 1996
B 1214

IVL

INSTITUTET FÖR VATTEN- OCH LUFTVÅRDSFORSKNING

SWEDISH ENVIRONMENTAL RESEARCH INSTITUTE

Organisation/Organization
Institutet för Vatten och Luftvårdsforskning

Adress/Address
P.O Box 47 086, 402 58 Göteborg

Telefonnr/Telephone 031-460080

RAPPORTSAMMANFATTNING
Report Summary

Projekttitel och ev SERIX projektnr

Rapportförfattare (efternamn, tilltalsnamn)
Author (surname, christian name)
Mellqvist, Johan; Arlander, Bill; Galle, Bo and Berqvist, Björn

Anslagsgivare för projektet/Project sponsor
Akzo Nobel Surface Chemistry AB
Borealis AB
Naturvårdsverket

Rapportens titel och undertitel/Title and subtile of the report

Measurements of Industrial Fugitive Emissions by the FTIR Tracer Method (FTM)

Sammanfattning/Summary

A new method called the FTIR Tracer Method (FTM), has been developed for measuring and quantifying fugitive (diffuse) emissions of hydrocarbons. The method has been evaluated in field experiments which were conducted in the vicinity of several petrochemical plants and an oil refinery during 1993-1995. The technique is based on concentration measurements with infrared remote sensing by Long Path Fourier Transform InfraRed (LPFTIR), combined with tracer releases. The field experiments show the FTM to be very useful for mass flux measurements of both alkanes and alkenes and that the measurements are consistent with the conventional SF_6 method. However, the technique needs to be further validated and a more thorough understanding of the measurement uncertainties have to be achieved.

Förslag till nyckelord samt ev anknytning till geografiskt område, näringsgren eller vattendrag/Keywords
Fugitive emissions, VOCs, FTIR

Bibliografiska uppgifter/Bibliographic data
IVL - publ.

Beställningsadress för rapporten/Ordering address
IVL, Biblioteket
Box 21060, S-100 31 Stockholm, Sweden

Summary

A new method called the FTIR Tracer Method (FTM), has been developed for measuring and quantifying fugitive (diffuse) emissions of hydrocarbons. This method has been evaluated in field experiments which were conducted in the vicinity of several petrochemical plants and an oil refinery during 1993-1995. The technique is based on concentration measurements with infrared remote sensing by Long Path Fourier Transform InfraRed (LPFTIR), combined with tracer releases.

The concentration measurements were performed up to a few hundred meters downwind of the diffuse leakages with reasonably high time resolution (1-6 measurements/minute). The source and tracer gases were measured simultaneously. If the tracer is released in the same location as the source gas then the ratio of the source and tracer gas will be constant and proportional to the mass flux of the source gas. In this study it is shown that it is sufficient with approx. 30 measurement points in order to obtain a reliable emission rate value. In order to remove outliers a weighted average is calculated over the 30 data points, where the weighting function is normalized and corresponds to the square of the tracer concentration. The parameter used to determine whether the source is well simulated by the tracer is the standard deviation of the ratio between the tracer and source gas. This standard deviation is weighted by the cube of the tracer concentration. The FTM technique works best in neutral meteorological conditions.

FTM measurements have been successfully conducted at 5 petrochemical process areas in Stenungsund. Most effort have been to perform measurements of ethylene, although measurements of both propylene and ammonia are demonstrated as well. The mass flux measurements of ethylene were performed on a range of sources with varying dimensions and leakage rates between 3 to 33 kg ethylene per hour. The concentration measurements were performed with long path FTIR technique, with different optical configurations and pathlengths. The distance from the source varied between 70 to 300 m. A comparison between the conventional SF_6 method and FTM indicates that the obtained leakage rates with the latter method are within the variability of the former method. The variability in the leakage rates obtained with the FTM have typically been in the order of 15%. The reason for this variability could be either real variations in the emission rates or measurement artifacts.

There have only been a few mass flux measurements of alkanes from crude oil tanks. The results show that the FTM is a useful technique for such measurements although it is more difficult to perform good tracer releases simulating the real leakages than in the petrochemical application. It is also more difficult to perform mixing ratio measurements of alkanes than of alkenes due to lower sensitivity of the available tracers and interfering absorption of water and other hydrocarbon species. FTM measurements on a crude oil tank with a floating roof showed emission rates of alkanes between 2 and 5 kg/h depending on the tank level and wind speed.

To summarize the field experiments show the FTM to be very useful for mass flux measurements of both alkanes and alkenes and that the measurements are consistent with the conventional SF_6 method. However, the technique needs to be further validated and a more thorough understanding of the measurement uncertainties have to be achieved. There is also a need for further software and hardware development of the FTIR systems.

1. Introduction

In this study we have investigated a method for measuring and quantifying fugitive emission of hydrocarbons. The work has been performed with support from several petrochemical industries in Stenungsund (*Borealis AB* and *Akzo Nobel Surface Chemistry AB*) from the *Swedish EPA* (Naturvårdverket) and the *Swedish OK Environmental Research Foundation* (OK Miljöstiftelse).

There is today an environmental need for developing techniques to quantify fugitive emissions (also called diffuse emissions) and the reasons for this will be discussed in the next chapter. Such techniques can be used to pin-point large emission sources, in order to reduce these further. Two industrial areas of particular interest when discussing fugitive emissions are refineries and petrochemical industries, from which a large amount of VOCs are emitted. Most of the emissions are diffuse and originate from leakages in pumps and valves and so forth. This means that there exists a vast number of emission sources, and it is therefore very difficult to quantify these emissions.

In a previous study (Mellqvist and Galle, 1994) the possibility of performing concentration measurements of hydrocarbons by remote sensing in the infrared region was studied. In this study such measurements have been incorporated in a methodology to quantify mass fluxes.

The developed methodology has been used to measure fugitive emissions from several industrial sites, such as a polyethylene production plant, a cracker plant for ethylene production, a ethylene oxide production plant, an amine production plant and an oil refinery. The main species emitted from the first three plants is ethylene, while ammonia is emitted in the amine production plant. In the refinery all measurement were made on crude oil tanks from which the main emitted species are light alkanes (C_2-C_7).

1.1. Environmental aspects of hydrocarbons emissions

The ozone concentration in the lower troposphere has shown an increase of 1-2% per year over the last 15 years (Staehelin and Schmid, 1991). A study by Bojkov (1986) indicates that the daily mean concentrations have doubled compared to concentration ranges estimated for the second half of the nineteenth century. These increased ozone concentrations have negative effects both on vegetation and on human health. The increasing background concentrations contribute to forest decline. Short term episodes with ozone mixing ratios exceeding 100 ppb can cause direct injuries to sensitive crops, e.g. spinach and potatoes.

In situ production of ozone in the lower atmosphere is thought to cause increase in the background concentrations (Crutzen, 1993). This is the result of several reaction paths including hydrocarbons, nitrogen oxides and sunlight. Methane together with CO is believed to be responsible for the increase of ozone in the free troposphere above the planetary boundary layer (altitude 1000-2000 m). Non methane hydrocarbons (NMHC) are on the other hand thought to be responsible for the ozone production below the boundary layer according to the following main reaction:

$$\text{NMHC} + NO_x + h\nu \rightarrow \text{secondary pollutants } (O_3, \text{PAN } ..) \quad (1)$$

This main reaction consists of a fairly large number of individual reactions. In the absence of NMHC the following reactions will take place (reaction. 2 and 3) , involving both the production and destruction of ozone (*thereby no net production*).

$$NO_2 + h\nu \rightarrow NO + O(^3P) \ (\lambda < 410 \text{ nm}) \quad (2)$$
$$O(^3P) + O_2 + M \rightarrow O_3 + M \quad (3)$$
$$O_3 + NO \rightarrow NO_2 + O_2 \quad (4)$$

In the presence of NMHC these will be converted to peroxy radicals ($\mathbf{R}CH_2O2$) by the reaction with OH and O_2 (reactions 5 and 6). The NO produced from reaction 2 can then be converted to NO_2 through reaction 7 and the OH radical will then be reformed according to the reactions 7 and 8. Reaction 7 will thus compete with reaction 4 for oxidizing the NO. *The net effect will be production of ozone.*

$$\mathbf{R}CH_3 + OH^{\cdot} \rightarrow \mathbf{R}CH_2^{\cdot} + H_2O \quad (5)$$
$$\mathbf{R}CH_2^{\cdot} + O_2 \rightarrow \mathbf{R}CH_2O_2 \quad (6)$$
$$\mathbf{R}CH_2O_2 + NO \rightarrow \mathbf{R}CH_2O + NO_2 \quad (7)$$
$$\mathbf{R}CH_2O + O_2 \rightarrow \mathbf{R}CHO + HO_2 \quad (8)$$
$$NO + HO_2 \rightarrow OH + NO_2 \quad (9)$$

The abundance of ozone in the lower troposphere in northern Europe is presently 30 ppb. The total European anthropogenic VOC emissions are 24.6 Tg/year (Sandnes and Styve, 1992) and approximately half of these are caused by traffic emissions. Sweden contributes to 1.2% of the total emissions (460 kton/year) of which 55% are caused by the traffic and the rest by industrial activities, for instance from refineries and petrochemical industries.

In Table 1 the lifetimes, average mixing ratios and photochemical ozone creation potentials (POCP) of several species are listed (Moldanova, 1994 and Andersson-Sköld and Pleijel, 1994). The POCP values below have been obtained by running a 4-day trajectory model assuming optimal conditions (sun) for ozone creation according to the reactions 1 to 9 above. Four days is a realistic time period during which optimal condition for ozone creation will prevail. In general alkenes (such as ethylene) have more impact on the O_3 production than alkanes.

Table 1. Yearly averages of hydrocarbon species at the Rörvik monitoring station 1989-1990 In addition the life time and potential for O_3 production is shown (Moldanova, 1994; Andersson-Sköld and Pleijel, 1994).

Species	Year average ppb	Lifetime (h)* sum./wint.	POCP (kg O3/kg Hc) *
C2H6	1.707	24/491	0.27
C3H8	0.732	5.6/115	1.09
i-C4H10	0.313	2.5/52	0.89
n-C4H10	0.545	2.7/56	1.02
i-C5H12	0.328	1.6/1.6	0.68
n-C5H12	0.241	1.6/1.6	
C2H4	0.598	0.8/15	2.18
C3H6	0.095	0.2/5	1.3

* Based on OH radical lifetime in standard air. ** 4 days calculation

Background levels of ozone

There are three important aspects about increasing background levels of ozone:

I) O_3 is a very efficient greenhouse gas and increased abundances cause changes in the radiative forcing of the atmosphere. It is quite difficult to calculate the impact that increased abundances of O_3 will have on the global warming since the impacts are dependent on the height distribution of ozone. If one assumes a homogenous profile than it can be shown that the production of ozone from 1 kg of emitted NMHC will have the same impact on the global warming as 8 kg of emitted CO_2 (IPCC, 1990).

II) There are strong indications that the increasing background concentrations of ozone may contribute to forest decline (Pye, 1989). The sensitivity of trees differs and in the US it has been shown that ozone has caused forest decline on several pine species. For Scandinavian spruce recent studies indicate that the danger of forest decline exists also in Scandinavia (Wallin, 1990).

III) O_3 is the main provider of OH radicals to the troposphere through the following reactions:

$$O_3 + h\nu \rightarrow O(^1D) + O_2 \ (\lambda < 315 \text{ nm}) \quad (10)$$

$$O(^1D) + H_2O \rightarrow 2\ OH \quad (11)$$

The importance of the OH radicals in the atmosphere lies in the fact that they react with almost all gases that are emitted by natural and anthropogenic sources, such as

hydrocarbons, CO, CH_4, NO, NO_2 and most sulfur and halogen containing species. It is actually the reactivity with OH that determines the atmospheric lifetime for most atmospheric species. The OH concentration in the atmosphere is thus strongly related to the O_3 concentration according to the reactions 10 and 11 and there are indications that increasing O_3 concentrations may have caused increasing OH concentrations in the beginning of the 1990's (Madronich, 1992).

To summarize the environmental danger in increased OH concentrations lies in the fact that it is extremely important in the atmosphere and that all concentration changes are negative, since they may induce other changes which in turn may change the chemical and radiative equilibrium of the earth. Secondly the abundance of OH is strongly coupled to the ozone formation (reaction 5). Higher reaction rates will decrease the lifetimes of the hydrocarbons and increase the O_3 production even more.

Ozone episodes
Under certain meteorological conditions (high pressure system, low wind speeds, southerly winds) there exist so called ozone episodes over Scandinavia. Continental "polluted" air which contains high mixing ratios of ozone formed from photochemical reactions of hydrocarbons and nitrogen oxides is transported to Scandinavia. Ozone mixing ratios as large as 120 ppb have been detected which induces a large stress on trees and plants, especially on clover and wheat (Pye, 1988; Pleijel, 1991).

Smog formation
In the vicinity of cities and other heavily polluted industrial areas with large concentrations of hydrocarbons and NO_x, photochemical smog will be formed according to reaction 1. The smog contains O_3 mixing ratios of several hundreds of ppb and other photochemical oxidants, such as PAN (peroxy acetyl nitrate), HNO_3, aldehydes and particles. The photochemical smog constitutes a serious health hazard and is today a large environmental problem in many cities and industrial areas.

1.2. Measurements of fugitive emissions

Due to the the reasons mentioned in the previous chapter there is an increasing concern to quantify fugitive emissions of gases from industrial processes, i.e. hydrocarbons from petrochemical industries, refineries and car production.

Such matters were discussed at a recent workshop on fugitive emissions held in Göteborg on the 29-30th of March 1995. Seventy participants from 11 countries were present, representing industry, the research community and governmental agencies. They were working with various activities such as: field measurements, leakage detection and reduction, instrument development and meteorology.

Among the conclusions from the industry were that measurements were needed in order to observe reduction efforts, and in order to develop better calculation methods for fugitive emissions. There exists presently no continuous measurement method for mass flux determination. Instead, the available methods can only be used in a semi continuous way.

A number of methods have been employed for estimation of fugitive emissions:

I. Chemical analysis of the concentration leeward of the plant in combination with dispersion models.

II. Tracer gas releases (SF_6) in combination with HC/SF_6 analysis with gas chromatography in a number of points downwind the plant(so called conventional SF_6 method).

III. Transections through the downwind plume using DIAL.

IV. Leak detection.

V. Calculation formulas.

I) In the first of these methods the concentrations of the emitted source gases are measured leeward of the plant. In order to estimate a mass flux, a Gaussian dispersion model is used.

This technique has been used by several groups in the US. They have been operating LPFTIR (Long Path Fourier Transform InfraRed) systems. The whole plume is traversed at some height by an infrared beam and then the integrated concentrations of the hydrocarbons can be evaluated. The distribution of the concentration in height is then calculated by dispersion modelling. Most of the work has been performed by consultants such as: *the Radian Corp.* in Austin, *Blasland Bouck & Lee* in New Jersey, *Environmetrics* in Texas and *Remote Sensing Air Inc.* in Missouri. The measurement systems are used also as first alert systems and for leakage detection.

The accuracy of the emission determination is strongly dependent on the applicability of the meteorological model used to determine the emission from the measured concentration. The problem is further complicated by the fact that the micrometeorology at industrial plants often is quite complex due to obstacles and temperature variations.

II) The second method is based on measurements of the ratio between a known "synthetic" emission (usually SF_6) and the gas under study (Sivertsen, 1983). If the tracer gas and the emission have the same source region and are spread in a similar way, the tracer replaces the meteorological model in the first described method, and from the ratio the emission can be directly derived. For the method to work it is necessary that the tracer is emitted in a way which resembles the emission to be studied. This is sometimes hard to accomplish. In order to verify similar source regions for the two gases a number of samples is collected at various locations downwind the plant. If they all show the same ratio the source simulation was successful. Thus for this method to work the source distribution has to be relatively well known, the meteorological conditions should be favorable and a number of samples have to be collected and analyzed. This method is employed by the Borealis process laboratory in Stenungssund on a regular basis and will further be refered to as the conventional SF_6 method.

III) The third method (DIAL) is based on laser absorption spectroscopy. Short pulses of light of different wavelengths are transmitted out in the atmosphere. The light backreflected from particles in the air is analyzed. The different absorption characteristics of different molecules in combination with time resolved detection electronics makes it possible to achieve range resolved concentration measurements of the species under study. Combined with wind data these concentrations can be integrated to yield the flux of the studied gas. The major drawback of this method is the complexity and cost of the measurement system, and thus the high costs for measurements. For this reason the described method can not be used continuously. The main uncertainties in the mass flux measurements originate from the estimation of the wind field rather than from the concentration measurement.

National Physical laboratory (NPL) in England has constructed several DIAL systems (Milton et al., 1992). These systems can measure NO, SO_2, O_3, benzene and toluene in the UV-range, NO_2 in the visible and methane and other hydrocarbons in the CH-stretch region (2.5-4-5 μm). They use a conventional dye laser and generate the infrared light by frequency mixing using a $LiNbO_3$ crystal. Such measurements require narrow bandwidths, high efficient light sources and low-noise-detectors due to inherent difficulties of measuring in the infrared region. Compounds that are measured in the IR region are propane, i-butane, n-butane, i-pentane and n-pentane. At the moment there exist three systems in Europe which all were developed by NPL. These are operated by NPL, Siemens together with Shell and Spectrasyne Inc.

The DIAL measurements utilize two different wavelengths, one which is absorbed by the hydrocarbons, λ_{on}, one which is not, λ_{off}. The difference in received intensities between the two wavelengths will be proportional to the hydrocarbon concentration. An example of a typical measurement region is shown in Figure 1.1, together with the absorbance spectra of ethane, butane and propane. Two potential wavelengths that can be used for DIAL measurements are shown. It can be seen that the absorbance of the three mentioned compounds overlap at the λ_{on} wavelength and the DIAL measurements will therefore measure the sum of the individual absorptions of each species emitted. The mixture of hydrocarbons at the measurement site therefore has to be well known. In the calibration procedure of the DIAL instruments a calibration spectrum for the

cocktail is obtained by adding the mixture compounds together in relation to their relative abundances.

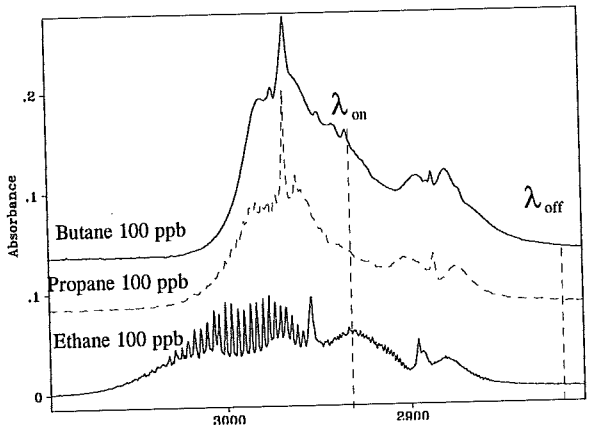

Figure 1.1. Example of the DIAL approach for concentration measurements. The absorbance spectra of ethane, propane and butane are shown together with potential frequencies for DIAL measurements.

IV) In the fourth method single leakages are detected. The concentration of the source gas is measured at the leakage point. The concentration can be converted to a mass flux by the use of empirical tables developed by the US/EPA. These have been developed by bagging typical process components and measuring their mass fluxes. By adding all measured leaks the total emission will be obtained. The leaks are identified with portable detectors but can also be found by trained dogs and this method is routinely used in several petrochemical industries.

V) The 5th method is widely used for determination of mass fluxes from tanks. The method is based on the use of calculation formulas developed by the American Petroleum Institute (API). These formulas predict mass fluxes on tanks as a function of various parameters. There have been little comparisons between the API models and real measurements and at the previously mentioned workshop held in Göteborg 1995, one of the conclusions was actually that such comparisons were needed.

2. Instrumentation

2.1 System for concentration measurements

2.1.1 Fourier Transform InfraRed (FTIR) Spectroscopy

The discovery of the Fast Fourier Transform in the 1960's and the availability of He-Ne lasers and mini computers in the 1970's made FTIR (Fourier Transform InfraRed) a recognized laboratory method for measuring high resolved spectra in the infrared (Griffiths, 1986). With the introduction of stable Michelson interferometers, sensitive semiconductor detectors and powerful PCs during the 1980's it has now become feasible to apply FTIR for open path measurements outside the laboratory, in the same manner as in the UV/Visible, (Axelsson, 1992).

In Figure 2.1 a commercial FTIR, Bomem MB-100, is schematically displayed. This instrument is rugged and stable and can be used outdoors, even in vibrating conditions. The spectrometer is of pendulum Michelson type and has a maximum resolution of 1 cm^{-1}. This resolution is satisfactory since the atmospheric line widths are of the order of 0.1 to 0.5 cm^{-1}. The detectors used in this study were a narrow band MCT (0.25 mm^2) and an InSb detector (1mm^2), depending on which wavelength range was studied. In such measurements, light is passed through the interferometer and then transmitted over the measurement distance to be analyzed by the detector. The light is thus modulated over the measurement distance, and the background radiation is suppressed.

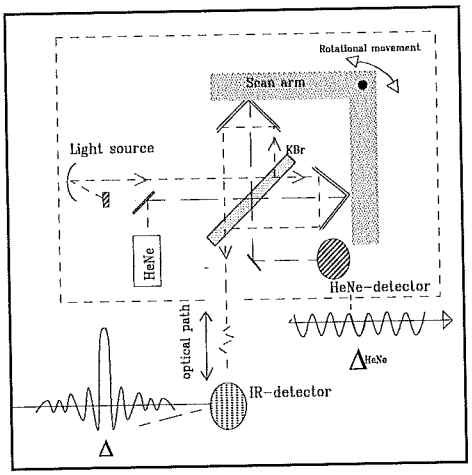

Figure 2.1. Schematic drawing of a Bomem MB-100 FTIR. The FTIR instrument is based on a modified Michelson interferometer which produces an interferogram. The interferogram is then converted to a intensity-wavenumber spectrum by an FFT-algorithm. The wavelength scale is internally calibrated by a He-Ne laser.

2.1.2 An open 1 km White system

In order to obtain long pathlengths, which improves the detection limit in absorption spectroscopy, there are several possible optical setups. In Figure 2.2 a custom made 1-km-open-White-system is shown , which is partly based on a concept by White (1942 and 1976). A more thorough description is given in Galle (1994).

Light from the internal spectrometer light source (glowbar) is split and recombined on the KBr beamsplitter and transmitted out of the instrument as a modulated beam with approximately 47 mrad divergence and diameter 25 mm. By means of two flat mirrors the beam is then entered into the multireflection cell via its entrance aperture. The slowly diverging beam is reflected in the right focusing mirror B2 (dia. 25 cm, f= 12.5 m) and focused back to spot 1 on the field mirror A (dia. 25 cm, f=12.5 m). After reflection in the left focusing mirror, B1, the beam is focused back to spot 2 on the field mirror. The light is reflected from point to point on the field mirror until it hits the exit aperture, point 20, and then the detector. Spot no. 5, 15 and 18 correspond to retroreflectors, consisting of two flat mirrors at right angle. The overall effect of the retroreflectors is to suppress mechanically caused beam displacements in both the vertical and horizontal directions.

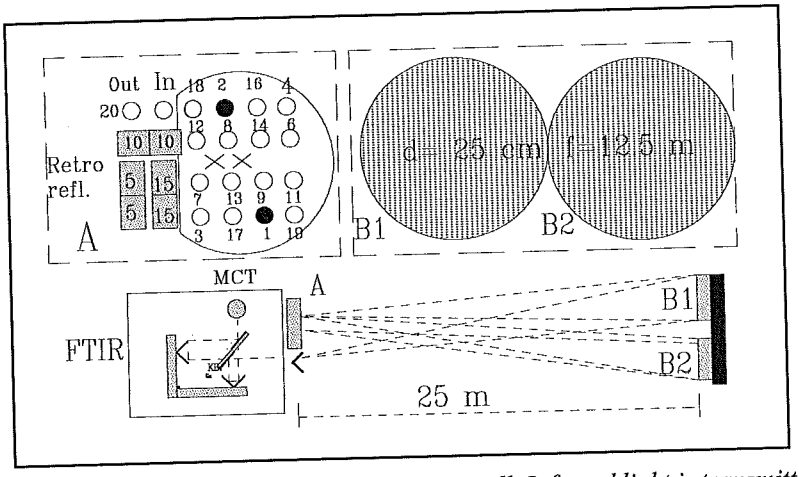

Figure 2.2. Schematic overview of an open path 1 km White cell. Infrared light is transmitted 40 times between the mirrors in the picture, separated by 25 m. An optical path of 1 km is thus obtained.

2.1.3 A single ended system

In Figure 2.3 a single ended Long Path FTIR system is shown. This system is an optional optical configuration to the one in Figure 2.2 and consists of a single Newtonian receiving/transmitting telescope, and a cubecorner array. In this system the light is transmitted a distance of 50 to 200 m and then reflected back by the cubecorner array. A single-ended system has the advantage that a large physical distance can be covered by the infrared beam, in order to traverse a whole emission plume.

The telescope is based on the use of a beam splitter (Ge) and only 25% of the light will therefore be used. In spite of this, the amount of light was quite high in the system in Figure 2.3. Due to the fact that MCT detectors become nonlinear at excessive light levels, an interference filter is used removing all wavelengths below 7.7 μm.

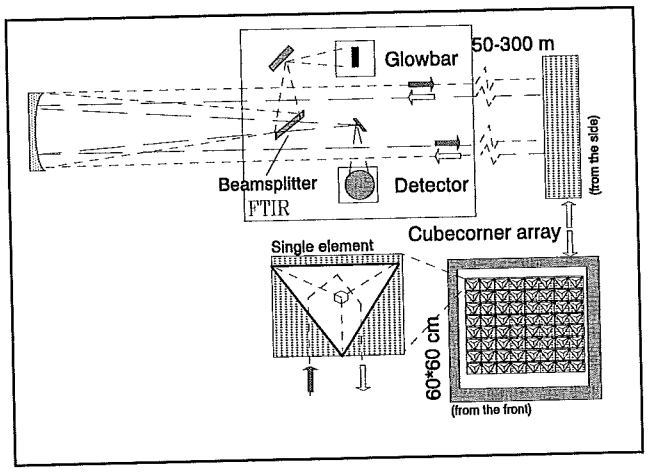

Figure 2.3. Schematic overview of a Long Path FTIR system.

2.1.4 Additional systems

Wind measurements

During the field experiments, the ground level wind speed and wind direction were measured with 4 anemometers from *Young* (Model 05103), coupled to a logger from *Campbell Scientific Ltd.*

Tracer gas release system

In the petrochemical application the main tracer used was SF_6. This species has virtually no background concentration in the atmosphere, it is inert and it has a large cross section in the infrared making it possible to use low flow rates in the tracer releases. The SF_6 was released at 6-9 locations inside the process areas by the use of individual gas cylinders. The individual mass flows were set equal by the use of flow regulators, 0.15-0.2 $kg \cdot h^{-1}$. The mass flow from each cylinder was calculated by weighing the gas cylinders before and after usage. The SF_6 tracer releases and weighing of the cylinders were performed by the *Borealis Cracker Laboratory*. They conduct such releases on a regular basis in order to obtain mass fluxes from the plant by the use of the conventional SF_6 method (described in section 1.2).

The main disadvantage with using SF_6 as a tracer in the petrochemical application, is that the absorption features of SF_6 and ethylene partly overlap (so called spectral interference). It was shown in the measurements that it was possible to overcome this interference by statistical evaluation methods. The main effect of the spectral interference however, is that the mass flow of the tracer has to be tuned to the amount of leakage of ethylene in order for the absorption features of SF_6 to not drown out the absorption features of ethylene. For instance, the SF_6 release rate was 2 $kg \cdot h^{-1}$ for an ethylene leakage of ca. 30 $kg \cdot h^{-1}$ and considerably less when the leakages were only 3 $kg \cdot h^{-1}$. Another potential tracer in some of the petrochemical applications is NH_3, although no satisfactory measurements were performed with this compound during this campaign.

For the measurements on the crude oil tanks at the Scanraff refinery we used tracers other than SF_6 due to the fact that another wavelength region was needed for the measurements of alkanes. N_2O and CO were tried as tracers. These gases have fairly high background mixing ratios in the atmosphere (N_2O~313 ppb and CO~160 ppb) and have weaker absorption cross sections than SF_6. High flow rates therefore had to be used (10 lit·min^{-1} of N_2O and 58 lit·min^{-1}of CO). The mass flows were calculated by using a flowmeter that was calibrated in the laboratory for the two species. In addition the consumption time of the gas cylinders were measured and these were consistent with the calibrated flow rates. The tracer releases were complicated at the crude oil tank measurements, since one was not allowed to put any equipment on top of the tanks. Instead long tracer release tubings had to be used (up to 50 m).
In Table 2 a summary of the tracer gases used in this study is shown.

Table 2. Tracer gases utilized in the field experiments at the petrochemical plants and at a refinery.

Species	Typical release rate (kg/h)	Application	Calibration	Absorption region (cm^{-1})
SF_6	0.5-2	petrochemistry	by weight	940-960
CO	4	refinery	calibrated flowmeter	2100-2200
N_2O	1	refinery	calibrated flowmeter	2170-2250

3. Method

The method employed, which we have called the *FTIR Tracer Method* (*FTM*), combines controlled releases of tracer gas with concentration measurements leeward of the diffuse leakages. The concentration measurements are conducted by Long Path Fourier Transform InfraRed (LPFTIR) spectroscopy which is a continuous infrared remote sensing technique. The FTM has been developed as a tool for studying and quantifying compound specific fugitive emissions with reasonable cost and effort.

3.1 Concentration measurements

The concentration measurements in this study were performed by an FTIR spectrometer coupled to different optical systems, as described in section 2. Broadband infrared light is transmitted through the atmosphere and then the obtained intensity spectra are analyzed. A thorough description on concentration measurement of molecules related to industrial activities (mainly hydrocarbons) have been described in two national reports (Mellqvist and Galle, 1994; Mellqvist, Arlander and Kloo, 1995).

The basis for the concentration measurements is that molecules absorb infrared light in a specific way. The absorptions correspond to energy transitions between different vibrational and rotational levels in the molecule and this yields absorption features which usually are unique for the molecule in question. This is especially true in the so called finger print region around 7-16 μm (600-1300 cm^{-1}) where compounds such as alkenes, ammonia and SF_6 are retrieved. In the CH-stretch region around 3-3.5 μm (2800-3300 cm^{-1}) the absorption features are much more similar to each other (especially large molecules and alkanes).

In absorption spectroscopy the Beer Lambert law has to be applied, Eq. 12. An exponential decay of the light intensity (*I*) exists for a specific wavelength (λ), when being transmitted a distance (*x*) through a gas containing an absorbing molecular species with a concentration (*c*). Here, σ corresponds to the absorption cross section which gives the probability for absorption. I_0 corresponds to a "clean air" spectrum which contains no absorption of the compounds to be measured.

$$I_t(\lambda) = I_0(\lambda) \cdot \exp(-\sigma(\lambda) \cdot c \cdot x) \tag{12}$$

$I_t(\lambda)$ = Detected light intensity, I_0 = Background intensity
σ = Absorption cross-section [cm^2/molecule] x = Optical measurement path [cm]
c = Number density of absorbing molecule [molecules/cm^3]

From the Beer-Lambert law the absorbance or optical depth (*OD*) can be derived, Eq. 13. The absorbance is directly proportional to the concentration and transmitted distance (*pathlength*) and the product of those two is usually called *total column* (c·x).

$$Absorbance = \log(\frac{I_0}{I_t}) = 2.3 \cdot c \cdot x \cdot \sigma = 2.3 \cdot OD \tag{13}$$

The absorption cross section σ is dependent on molecular species, wavelength, temperature and pressure. There exists spectral libraries in the infrared spectral region

which contain information on the absorption cross sections (linestrength, linewidth and other molecular parameters), making it possible to simulate absorption spectra for a typical instrument at various conditions (temperature, pressure, concentration).

The most common data base is the *High-resolution transmission molecular absorption* data base, with the acronym HITRAN (Rothman et al., 1992). It covers the absorption lines for the 31 most abundant molecular species in the atmosphere. In this study we have used HITRAN for the spectral evaluation of CO, N_2O, H_2O and NH_3. A software package called SALT by Griffith(1995) has been used to convert the HITRAN linestrengths to FTIR spectra at a resolution of 1 cm^{-1}.

Another spectral library is provided by Hanst (1990). It contains absorbance spectra measured at 1 cm^{-1} resolution for a large number of species. Here we have used this library for the spectral evaluation of alkanes, alkenes and SF_6.

A 3rd spectral library is provided by the US EPA (NIST/EPA). It contains spectra of approx. 4000 species at a slightly lower resolution than used in this study, 4 cm^{-1}. This library is however qualitative and provides solely the spectral features (finger prints), thus making it unsuitable for absolute measurements of species. In this study the library has been used to get a qualitative idea of the constituents in the vapor from the crude oil.

To obtain concentrations from the measured intensity spectra the following steps are conducted:

I. Measurement of an intensity spectrum.
II. Conversion to an absorbance spectrum by the use of Eq. 13. In this study the I_0 spectra were chosen as the spectra containing the smallest amount of tracer or source gas from a specific measurement site and period.
III. The absorbance spectrum is then fitted to a calibration absorbance spectrum obtained from one of the libraries mentioned above. The fitting is performed by a statistical least square method called CLS (Classical Least Square). This is done in a commercial software package called LabCalc by *Galactic Inc.* From the spectral fitting procedure the scaling factor between the calibration and measured absorbance spectrum is obtained. The total column of molecules in the measured spectrum is then simply the scaling factor multiplied by the total column in the calibration spectrum. In the spectral fit the standard deviation between the two spectra is also calculated and this is a good indicator for the quality of the fit.

3.1.1 Spectral features

In Figure 3.1 the spectral region is shown which have been used in this study for measurements of chemical species in vicinity of several petrochemical plants in Stenungsund. The finger print region is used in which the species have quite unique features.
Absorbance spectra from Hanst (1990) of ethylene, propylene and sulfurhexafluoride are shown together with a measured absorbance spectrum from the Borealis cracker, containing 10 ppb ethylene, 34 ppb propylene and 0.3 ppb SF_6. The negative peaks correspond to water, which is more abundant in the reference spectrum used. It can be seen that water absorbs in the vicinity of both SF_6 and propylene. In this study the I_0 spectrum (Eq. 13) were chosen as the "cleanest" spectrum in a measurement set of 30

to 60 spectra. Over the time period of these spectra (5 min. - 1 h) the water concentration in the atmosphere were fairly constant and therefore most of the water absorption was removed by normalization with the I_0 spectrum according to Eq. 13. In the spectral evaluation procedure in this study calibration spectra of water, ethylene and SF_6 was fitted to the measured absorbance spectra.

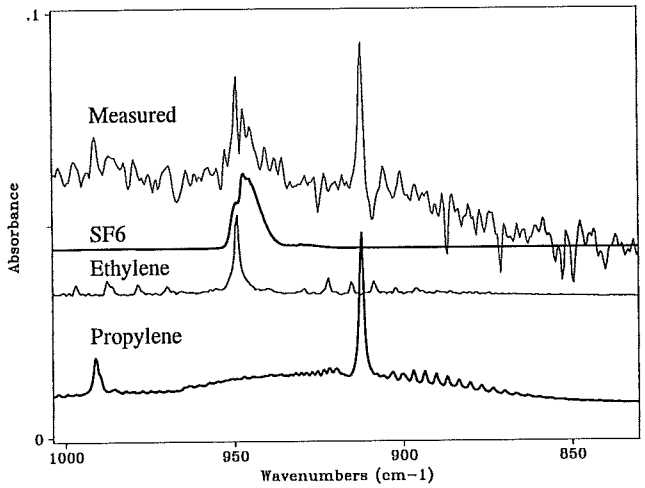

Figure 3.1. Measured absorbance spectra from the Borealis Cracker containing ethylene(10 ppb), propylene (34 ppb), and SF_6 (0.3 ppb). The calibration spectra of the three species are also shown.

At the *Scanraff refinery* concentration measurements were performed on hydrocarbons leaking from crude oil tanks. The mass composition of a typical crude oil vapor (Corinair, 1994) is shown in Figure 3.2. The species are mainly alkanes and these are measured by utilizing their absorption features in the CH-stretch region around 3-3.5 μm (2800-3300 cm^{-1}).

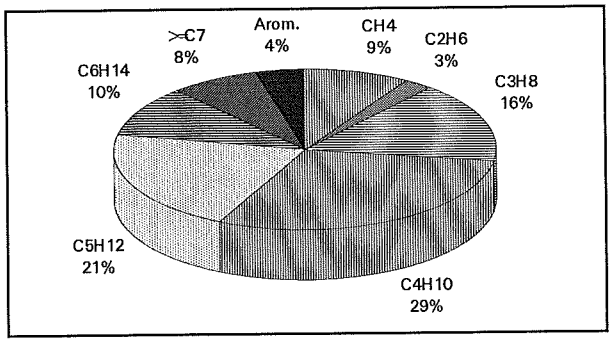

Figure 3.2. Weight composition of Crude petroleum vapor (Corinair, 1994).

In Figure 3.3 (a) and (b) absorbance spectra of alkanes are shown from C_3 to C_{10}. These spectra were obtained both from the Hanst (1990) library as well as the qualitative NIST/EPA library. It can be seen that the features of the lighter species differ most. It can also be seen that the absorbance increase at the peaks as a function of carbon number. It is only to the left in Figure 3.3 (a) that the situation is reversed. A good indicator of heavy hydrocarbons is the relative magnitude of the middle peak around 2937 cm^{-1} compared to the peak around 2970 cm^{-1}.

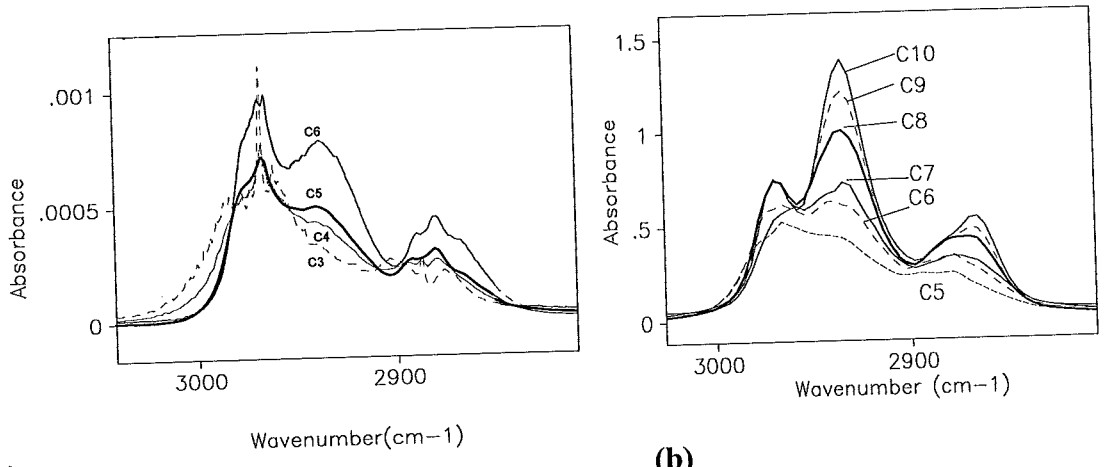

Figure 3.3. a) The absorbances (1 cm^{-1} resolution) for 1 ppb each of the alkanes C_3-C_6, (pathlength 1 km) obtained from (Hanst, 1990). b) The absorbances (4 cm^{-1} resolution) for arbitrary concentrations of the alkanes C_5-C_{10}, obtained from (NIST/EPA).

From the discussion above it can be understood that absorbance spectra of crude oil vapor will correspond to several overlapping absorptions in the CH stretch region. The total absorbance will correspond to the one of the average molecule, *the cocktail molecule*. Based on the Corinair(1994) data shown in Figure 3.2 a cocktail spectrum was constructed. Due to the fact that alkanes larger than C_6 were not included in the Hanst (1990) library, a cocktail spectrum was simulated, with the relative amounts as shown in Figure 3.4. The cocktail molecule has an average carbon number of 4 with a molecular weight of 57.9.

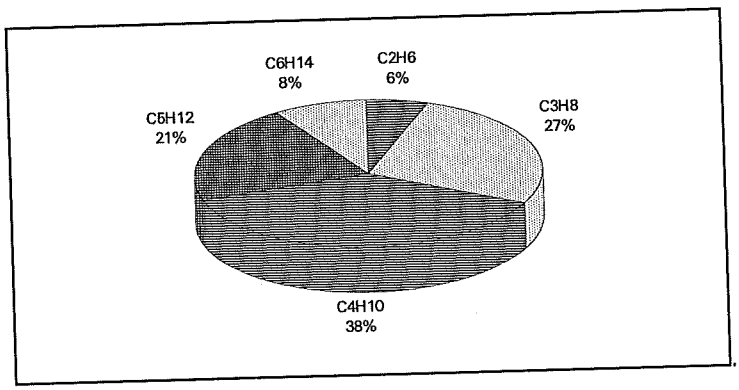

Figure 3.4. Relative amounts of hydrocarbons in the hydrocarbon cocktail based on the Corinair (1994) data.

In Figure 3.5 a measured spectrum from the crude oil is shown (*measured*) together with the absorbance spectra of the cocktail and of hexane. It can be seen that the measured spectrum is much more similar to hexane than to the cocktail spectrum, indicating that the true cocktail consists of considerably heavier alkane species than what is given by the Corinair (1994) data. A comparison of the absorbance magnitudes shows that the measured spectrum corresponds to a total column of 31.2 ppm·m (110 mg/m^2) of hexane or 46.9 ppm·m (111 mg/m2) of the cocktail molecule.

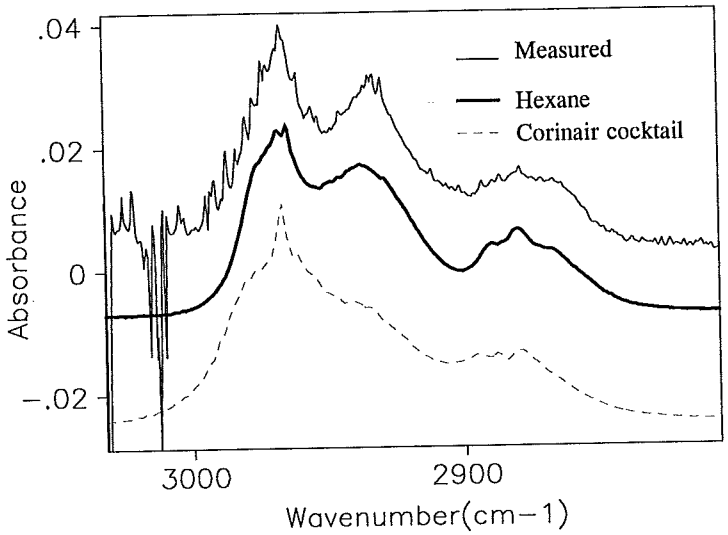

Figure 3.5. Measured crude oil spectrum together with absorbance spectra of the cocktail (Corinair, 1994) and of hexane. The measured spectrum correspond to a total column of 31.2 ppm·m of hexane or 46.9 ppm·m of the cocktail molecule.

3.2 Methodology

The FTM is based on the use of tracers (e.g. SF_6, CO, N_2O, NH_3). These are released in a controlled manner near the supposed locations of the diffuse leakages. For the method to work it is important that the tracers mix with the leaking gas (source gas) inside or in the vicinity of the source. In Figure 3.6 (a) and (b) typical areas for leakages are shown. In Figure 3.6 (a) the leakages occur on top of an oil tank. Tracer gas is released on top of the tank and then the tracer and source gas will mix, both on top of the tank and behind in the wake. The gases are then transported downwind in a gaussian manner. In Figure 3.6 (b) the meteorological situation at a typical petrochemical process area is shown. Tracer gas is here released windward of the process area where the leakages occur. The source and tracer gas are then mixed inside the structure.

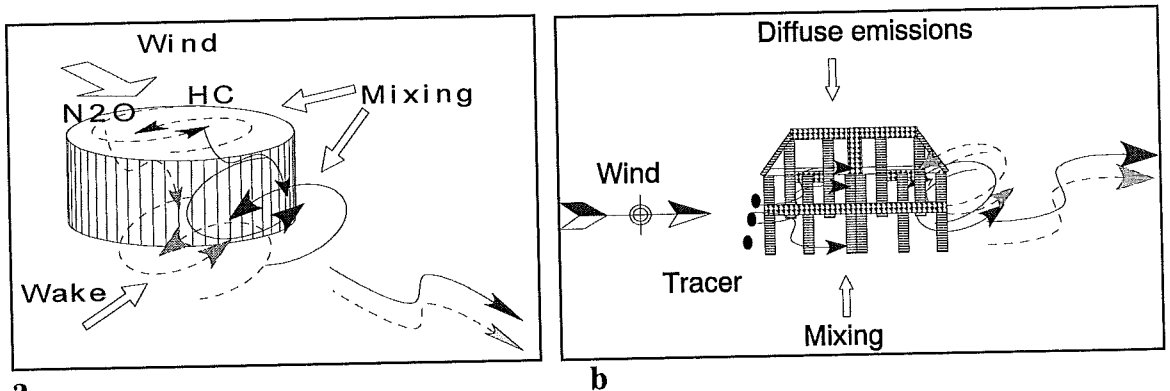

Figure 3.6. a) A schematic overview over the wind fields in the vicinity of a crude oil tank. The emissions occur on top of the tank.
b) A schematic overview over the wind fields in the vicinity of a typical petrochemical process area.

In the FTM the concentrations of the tracer and source gas are measured continuously downwind the leakage by FTIR (Fourier Transform InfraRed) spectroscopy. If the tracer gas emissions simulate the source gas emissions well, there will be a correlation

over time between the two gases. The ratio in the mixing ratios of the source and tracer gas will then be proportional to the mass flux of the source gas according to Eq. 14.

$$\Phi_{source} = \frac{N_{source}}{N_{tracer}} \cdot \frac{M_{source}}{M_{tracer}} \cdot \Phi_{tracer} \tag{14}$$

where Φ corresponds to the mass flux, N to the mixing ratio and M to the molecular mass.

If one assume that the tracer releases simulate the source gas emissions well, the next problem is the removal of outliers. In the FTM an approach has been chosen in which a weighted average over the obtained mass fluxes is calculated. The weighting function, F(t), is normalized and corresponds to the square of the tracer concentration. Mass fluxes obtained during high tracer concentrations will therefore dominate in the averaging procedure. Eq. 15 and 16 yields the weighted average over the time period t_1 to t_n.

$$\overline{\Phi}_{source} = \sum_{t1}^{tn} F(t_i) \cdot \Phi_{source}(t_i) \tag{15}$$

$$\text{where } F(t_i) = \frac{N_{tracer}(t_i)^2}{\sum_{t1}^{tn} N_{tracer}(t_i)^2} \tag{16}$$

A good criteria for determining whether the source simulation is adequate, is that the derived emission rates from Eq. 14 should be constant during periods with high tracer concentrations, assuming a constant emission. This can be obtained by calculating a tracer weighted standard deviation, Eq. 17 and Eq. 18. In this study a normalized weighting function has been used which is proportional to the cube of the tracer concentration.

$$STD = \sqrt{\sum_{t1}^{tn} F_{std}(t_i) \cdot (\Phi_{tracer}(t_i) - \overline{\Phi}_{source})^2}\,, \tag{17}$$

$$\text{where } F_{std}(t_i) = \frac{N_{tracer}(t_i)^3}{\sum_{t1}^{tn} N_{tracer}(t_i)^3} \tag{18}$$

The number of points (n) in the averaging procedures in Eq. 15 and Eq. 17 should be chosen long enough to obtain a statistically significant number of data points, but shorter than the time by which the emissions are expected to vary. In this study we have chosen a number of 30 data points as the critical amount and depending on the integration time of the measurements this corresponds to a time interval between 5 to 30 minutes.

The reason for performing a weighting procedure with the tracer concentration is to remove outliers. Greatly overestimated emission values will be obtained from Eq. 14 in cases when other sources blow into the beam and the tracer concentration is small. In the weighting procedure in Eq. 15 the square of the tracer concentration is multiplied by the derived mass flux, which is inversely proportional to the tracer concentration. Each term in Eq. 15 will thus be directly proportional to the tracer concentration. Mass flux values obtained when the tracer is small will therefore affect the average value very little.

In the calculation of the standard deviation in Eq. 17 the cube of the tracer concentration is multiplied by the quadratic difference between the weighted average and the single derived mass fluxes. The second factor is inversely proportional to the square of the tracer concentration. Each term in Eq. 17 will therefore be directly proportional to the tracer concentration, in consistency with the weighting procedure in Eq. 15.

The mixing ratios of ethylene (source) and SF_6 (tracer) are shown Figure 3.7 (a). These were measured over a 100 m optical path at distance of 180 m from a process area in a plant in Stenungsund. The mixing ratios were obtained by calculating the absorbance according to Eq. 13, and then fitting these to calibration spectra as described in section 3.1. A spectrum which appeared to have a low absorption of both the tracer and source gas was chosen as the I_0-spectrum. In Figure 3.7 (a) the spectrum measured around 15:40 was chosen as the I_0 spectrum.

In Figure 3.7 (b) the ethylene is shown versus the SF_6. Such a graph gives direct information about the measurement situation. If the graph doesn't go through the origin this can be caused by several things and this will be further discussed below. If the correlation between the tracer and source gas is bad this can caused by bad simulation of the source by the tracer (the tracer releases are not performed close enough to the VOC leakages). A bad correlation can also be caused by time variations in the emission rates. Which of these that is applicable can be revealed by a study of the time series in the derived emission rates in relation to meteorology and process activities.

In Figure 3.7 (c) the time series of the derived emission rate of the source gas is shown, obtained according to Eq. 14. In addition the tracer mixing ratio is shown. It can be seen that when the tracer value is high the emission rates are quite constant. The tracer weighted average corresponds to 15 kg(C_2H_4)/h and the standard deviation is 19%.

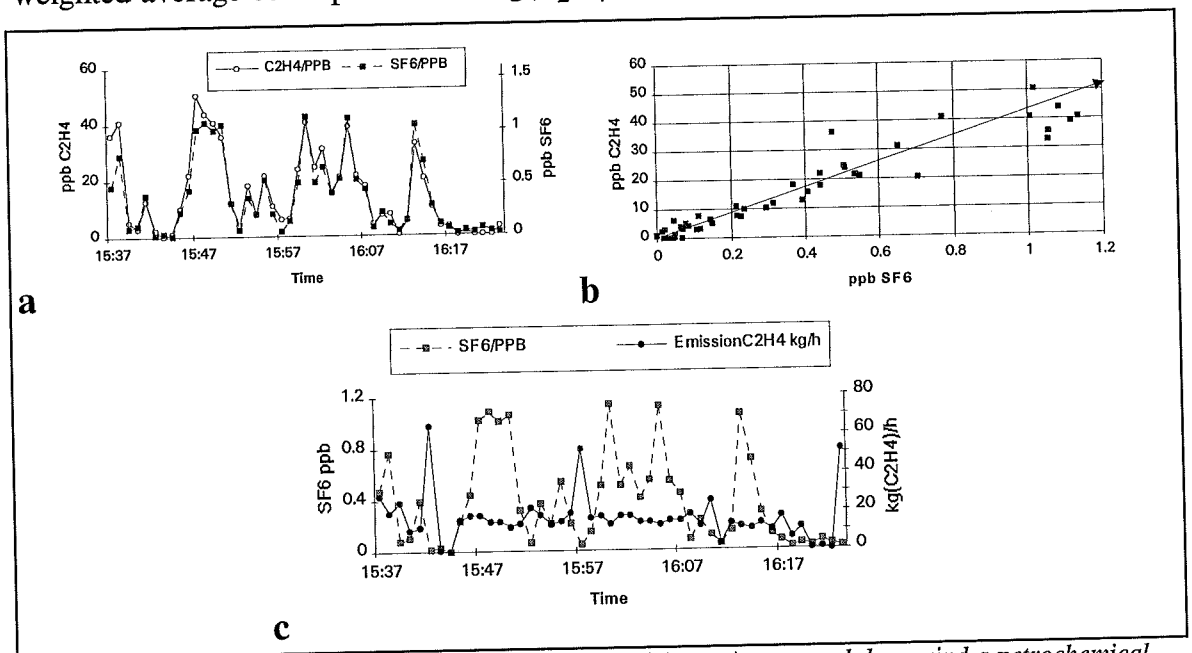

Figure 3.7. a) Mixing ratios of ethylene (source) and SF6 (tracer) measured downwind a petrochemical plant (Borealis Cracker). b) Scatter plot of the time series in Figure A. c) SF_6 mixing ratio and calculated emission of C_2H_4 as a function of time.

In Figure 3.8 plots are shown of the source versus the tracer concentration. These are hypothetical but represent typical cases that can occur when performing FTM measurements. In case A there is a negative offset on the tracer gas axis. This implies that the I_0 spectrum used (see section 3.1) contains a significant amount of absorption from the tracer gas. A measured spectra containing less tracer gas absorption will therefore yield a negative absorbance (and concentration) when normalized with the I_0 spectrum according to Eq. 13. In case B the correlation has a negative offset on the source axis. This implies that the I_0 spectrum used contains absorption from the source gas. In case C the correlation has a positive offset on the source axis. This implies that there is a constant background present of another source which does not correlate with the tracer.
All concentration values were compensated for the offsets shown in the cases in Figure 3.8 and case B was the most common. In most cases no compensation was needed however since it was possible to find a I_0 spectrum containing neither source nor tracer gas in a measurement set of 30 to 60 data points.

The general methodology for the FTM is summarized in Table 3.

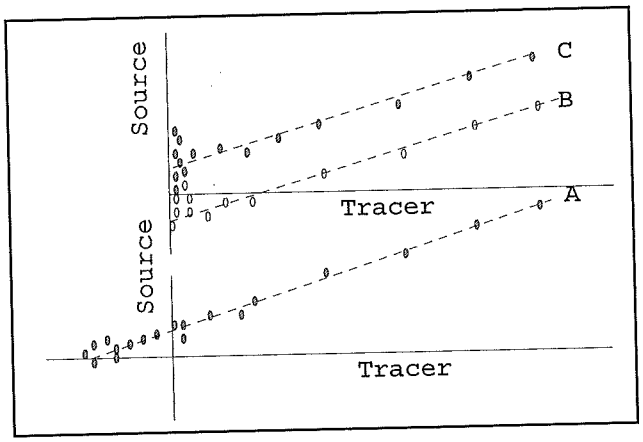

Figure 3.8. The source versus the tracer concentration in three typical and arbitrary measurement situations. In case A the correlation has a negative offset on the tracer axis. This implies that the I_0 spectrum used contains tracer concentration. In case B the correlation has a negative offset on the source axis. This implies that the I_0 spectrum used contains source concentration. In case C the correlation has a positive offset on the source axis. This implies that there is a constant background concentration from another source present which does not correlate with the tracer.

Table 3. The methodology used for the FTM.

Methodology
1. One or several tracer gases are emitted from several cylinders positioned at typical locations for leakages inside the process area to be studied.
2. Infrared absorption spectra are recorded by FTIR at a distance of 100 to 300 m downwind the emission source. The spectra are recorded over a distance of 25 to 200 m with a time resolution of 1-6 spectra/minute.
3. The concentration of the tracer and source gas are retrieved from the recorded spectra. The intensity spectra are converted to absorbance spectra by dividing with a spectrum (I_0) containing the lowest concentration of the source gas. The concentrations are obtained by spectral evaluation of the recorded absorbance spectra to calibrations spectra.
4. A tracer weighted average of the emission value is calculated for a certain amount of measurement points (30) according to Eq. 14, Eq. 15 and Eq. 16.
5. The source simulation by the tracer is quantified by calculation of the weighted standard deviation according to Eq. 17 and 18.

3.3 Meteorological discussion

The local meteorology is very complex in the vicinity of process areas and oil tanks as was illustrated in Figure 3.6. This makes it complicated to use models for mass flux estimation. However models can be used to estimate the dimensions of the emission plumes and from this suitable optical paths for LPFTIR measurements can be chosen. Models can also be used to validate theoretically inherent uncertainties in the methodology.

In general there are large turbulent eddies in the vicinity of constructions. Downwind, airparcel travels in a Gaussian manner, according to Eq. 19.

$$C(x,y,z) = \frac{2}{\pi} \cdot \frac{Q}{u \cdot \sigma_{y(x,S)} \cdot \sigma_{z(x,s)}} \exp\left(-\left(\frac{y^2}{2\sigma_{y(x,S)}^2}\right) - \left(\frac{z^2}{2\sigma_{z(x,S)}^2}\right)\right) \qquad (19)$$

here C corresponds to the concentration downwind. Q is the source strength [g/s], u is the wind speed [m/s] (x-direction), σ is the standard deviation in the vertical (σ_z) and horizontal direction (σ_y). The parameter σ is dependent on the distance from the source and the local meteorology, such as the wind speed. A property of the Gaussian distribution is that 95% of the mass will be confined within $\pm$ 1.96·σ.The meteorology is given by an empirical and discrete parameter (*S*) called stability class. It can have several values from A to F. A corresponds to unstable conditions with low wind speeds (<2 m/s) and large solar radiation, while D corresponds to neutral conditions with moderate sun and wind speeds above 6 m/s. The wind field is assumed to be uniform.

Typical plume widths (containing 95% of mass) down wind from a point source are shown in Figure 3.9 at neutral (D) and unstable conditions (A). Turbulence around solid structures broadens the plume. The magnitude of the broadening will be in the same order as the size of the structures creating the dispersion.

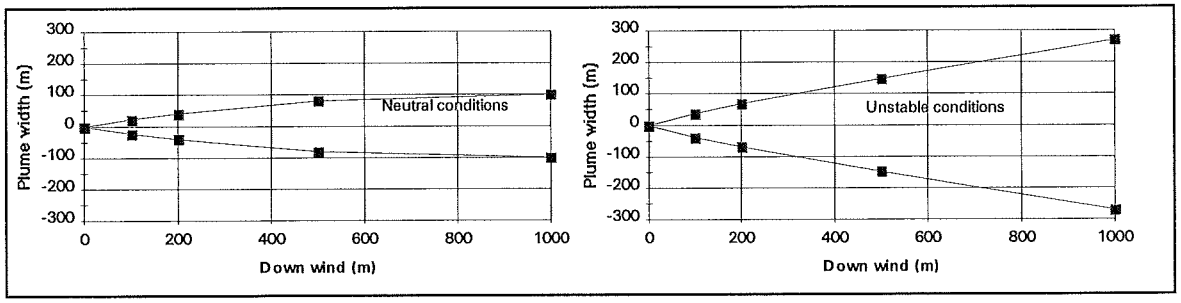

Figure 3.9. Plume width on the ground (95% of the mass) as a function of distance downwind the source. Neutral and unstable conditions are shown conditions.

A model based on Eq. 15 has been developed by the US EPA (Screen 2)[1]. In the model it is possible to simulate point, area and volume sources. The model was used to

[1]Screen 2: "Screening Procedures for Estimating the Air Quality Impact of Stationary, Sources, Revised," EPA-450/R-92-019

simulate typical Gaussian plumes for the process areas under investigation in the field campaigns. The results from such simulations are shown in section 4.

In addition the screen 2 model was also used to get an idea of the uncertainties involved in the FTM technique. What was interesting to investigate was how much error would occur if the mixing of the tracer and source gas would be purely Gaussian.

A typical case was assumed in which two point sources with equal source strength were separated by 30 m. In Figure 3.10 such a case is shown in which one of the two point sources correspond to the tracer and the other to the source gas. In the simulation unstable conditions were assumed and a distance of 300 m from the sources was studied. The concentration and ratio between the source and tracer gas are shown over the cross section of the plume. It can be seen that in this case the ratio is only correct in the middle of the total plume and even 25 m from the center the error will be 30%.

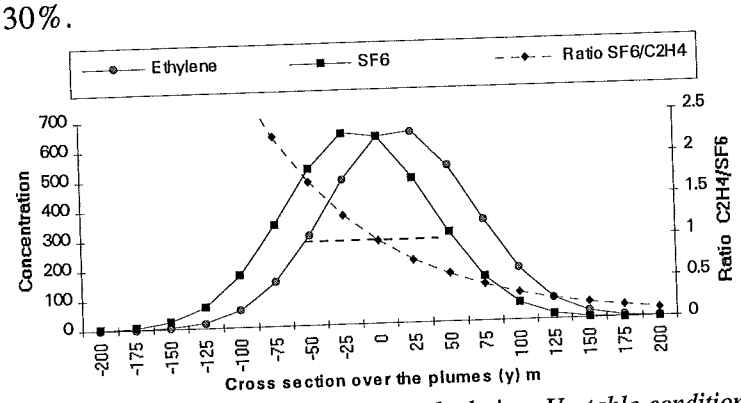

Figure 3.10. Gaussian point source calculation. Unstable condition 3 m/s

A similar simulation was performed in which both the tracer and the source gas were assumed to be released at two locations separated by 30 m. The relative source strengths of the tracer and source gas source were assumed to be different however. This is rather typical for the source simulations in the field experiments performed in this study. The tracer was released at several locations in the process area with the same mass flow in every location. The leakages of the source gas on the other hand varied from location to location.

In Figure 3.11 the concentration of the tracer and source gas has been simulated over the cross section of the plumes of the tracer and source gas, 300 m downwind the emissions at unstable conditions (sun, 3 m/s). In addition the tracer/source ratios over the cross section of the plume are shown and the theoretical ratio. The emission of the tracer (SF_6) was 10 g/s at both locations. The source emission was 10 g/s at location 1 (+15 m), and 5 g/s at location 2 (-15 m). In Figure 3.12 (b) the relative error in the tracer/SF6 ratio as obtained by long path measurements over 100 m and point measurements respectively are shown. The data in Figure 3.13 are the same as in Figure 3.12 although at neutral conditions (mod. sun, 10 m/s).

In these particular simulations assuming purely Gaussian conditions it can be seen that the tracer/source ratios are correct in the middle of the two sources (y = 0), while the ratio deviates up to 50% at the sides. It can also be seen that the long path measurements are less sensitive to correct position than the point measurements.

One conclusion from these simulations is that under Gaussian conditions the ratio will be more correct in the middle of the plume than in the outskirts. In the FTM method we applied SF_6 weighting meaning that the ratio obtained will correspond to the middle of the SF_6 plume.

In real world measurements the situation will be better since most of the mixing actually should occur inside the process area. The SF_6 should for this reason always be emitted in the windward side so that the tracer will blow through the process area.

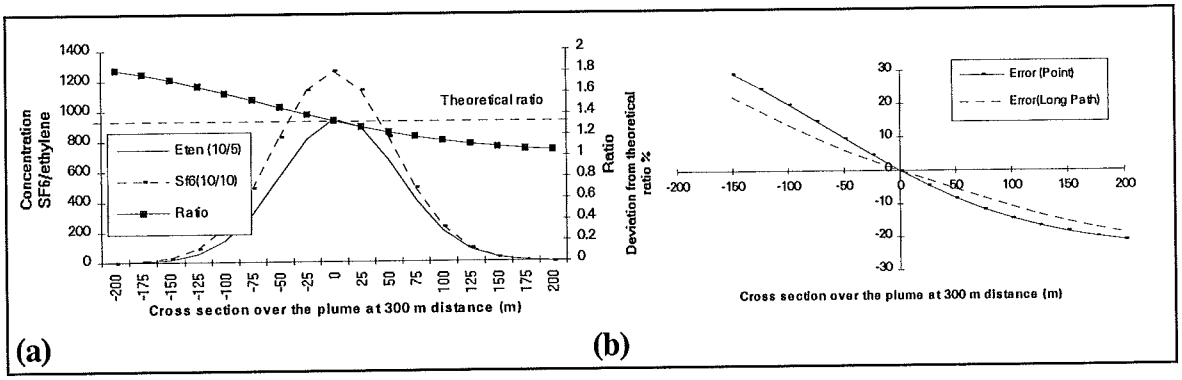

Figure 3.11. a) Concentrations of the tracer and source gas over the cross section of the plumes, 300 m downwind the emissions (unstable conditions (sun, 3 m/s). The emission of the tracer (SF_6) was 1 g/s at both locations. The source emission was 1 g/s at location 1 (+15 m), and 0.5 g/s at location 2 (-15 m). The tracer/source gas ratio is also shown together with the theoretical ratio.
b) The relative error of the tracer/soure gas ratio over the cross section of the plume. Relative deviation of the data shown in the previous figure. Long path measurements over 100 m are compared to point measurements.

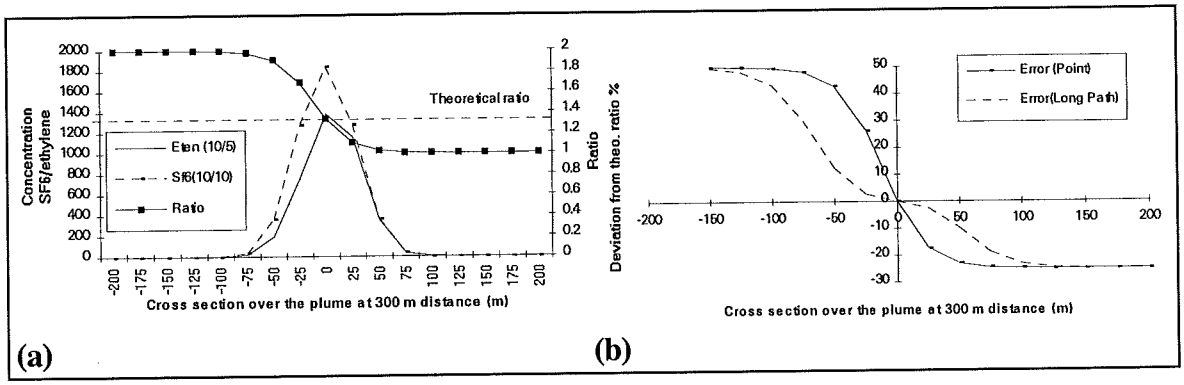

Figure 3.12. a) Cross section over the plumes of the tracer and source gas 300 m downwind the emissions at neutral conditions (mod. sun, 10 m/s). The emission of the tracer (SF_6) was 10 g/s at both locations. The source emission was 10 g/s at location 1 (+15 m), and 5 g/s at location 2 (-15 m).
b) Relative deviation of the data shown in the previous figure. Long path measurements over 100 m are compared to point measurements.

4. Field experiments

Field experiments were performed during the period 1993 to 1995, at four plants in Stenungssund (*the Borealis Cracker plant*, the *Borealis polyethylene plant*, the *Akzo Nobel ethylene oxide plant*, the *Akzo Nobel amine plant*) and the *Scanraff refinery* in Lysekil, in the south western part of Sweden. In these experiments the FTM was evaluated. The measurements were conducted with the systems described in section 2.

4.1 The reactor area at the Akzo Nobel EO plant

Ethylene oxide is produced from ethylene and oxygen at the EO plant of Akzo Nobel Surface Chemistry. The two raw compounds react under enhanced pressure and temperature in a catalytic reactor system. The production of ethylene oxide is approx. $6.5 \cdot 10^3$ kg/h. The main VOC being emitted from the plant is ethylene and it is estimated[2] by calculations that the diffuse leakage from the whole plant is less than 13 kg/h.

FTM measurements were performed in the end of August 1994 at the EO plant. The main VOC leakages are believed to be in the vicinity of the reactor area, which is rather small and has the approximate dimensions: height 10 m, base length 30 m and width 10 m. Six SF_6 cylinders were placed at different locations in the process area, each with a mass flow of 0.12 kg/h. Four of the cylinders were placed at the ground level, while one cylinder was placed at the first level (5m) and the last cylinder at the top level (10m). FTM measurements were then performed at two locations, pos. 1 placed 60 m west of the reactor and pos. 2 placed 150 m northwest of the reactor, Figure 4.1.
The FTM measurements were performed with the open 1 km White system described in section 2. Initially we tried to conduct mass flux measurements of both ethylene and ethylene oxide. The concentration of the latter species was below the detection limit of 3.5 $\mu g/m^3$, however.

In Figure 4.2 the Gaussian parameters for the plume from the reactor are shown. The measurements at the reactor were performed at neutral conditions (D) with wind speeds around 8 m/s at 10 m elevation and overcast conditions. The wind speed at the ground, leeward of the emission source, was considerably lower (2.5 m/s). It can be deducted from Figure 4.2 that at a distance of 150 m, 95% of the plume mass at the ground level will be confined within 80 m.

---

[2]Environmental report, 1994

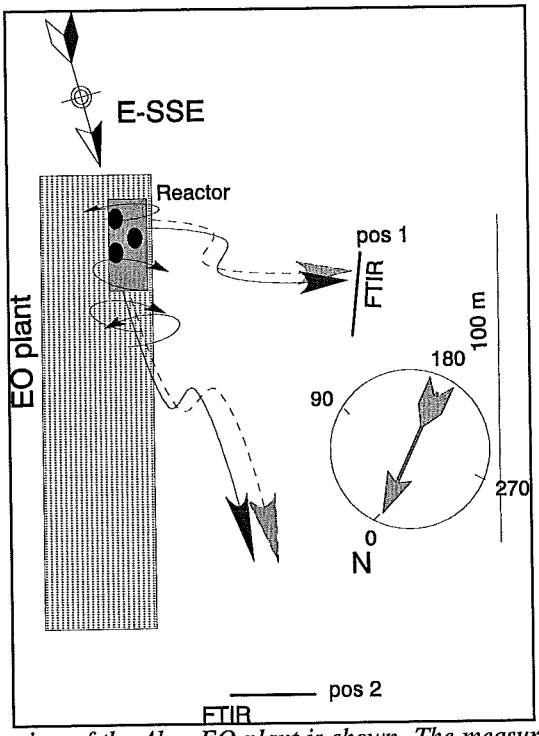

Figure 4.1. A schematic overview of the Akzo EO plant is shown. The measurements were performed at two positions at a distance of 65 m and 150 m, respectively, from the reactor.

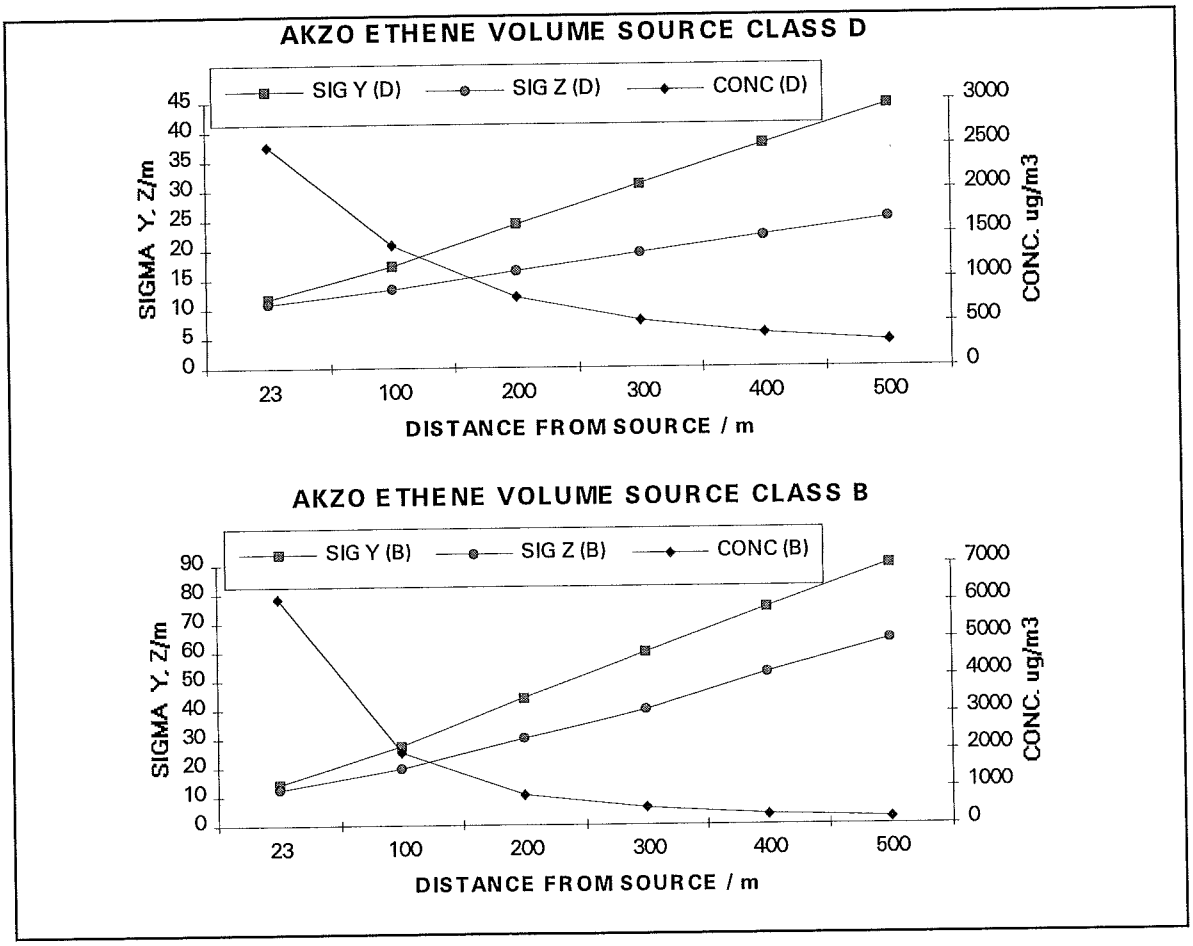

Figure 4.2. Gaussian plume parameters for the reactor at two stability classes, neutral (D) and unstable(B).

In Figure 4.3 the FTM measurements at position 1 are shown, conducted at a time resolution of 1 measurement/minute. The mixing ratios of SF_6 and ethylene are plotted versus time in Figure 4.3 (a). In Figure 4.3 (b) these mixing ratios have been plotted versus each other showing a ratio of (43:2). In Figure 4.3 (c) the emission rates derived by Eq. 14 are shown together with the tracer mixing ratio (SF_6). It can be seen that when the tracer is high the ratio is fairly constant. The tracer weighted average emission corresponds to 2.8 kg/h with a standard deviation of 18%.

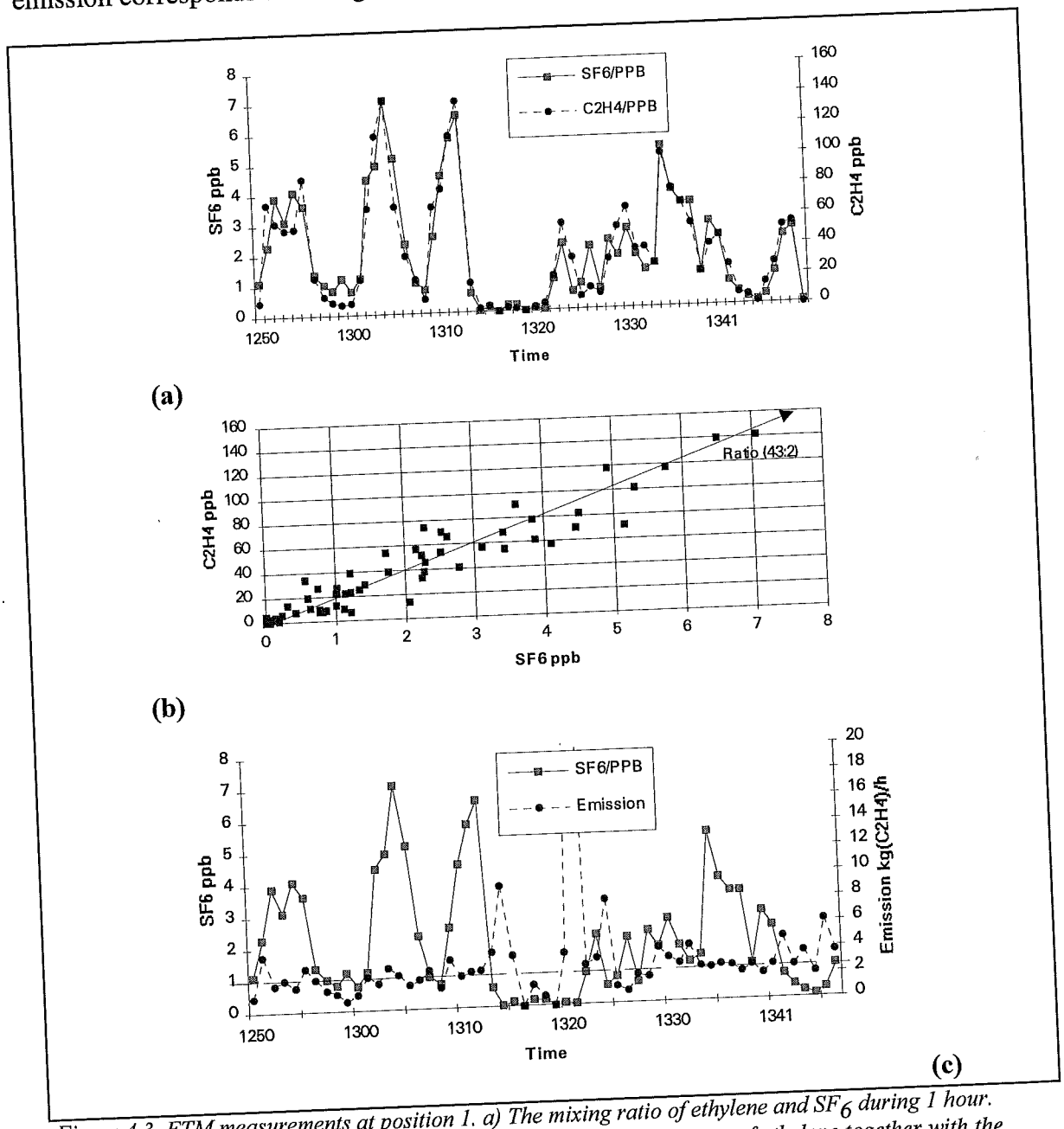

Figure 4.3. FTM measurements at position 1. a) The mixing ratio of ethylene and SF_6 during 1 hour. b) The mixing ratio of ethylene versus SF_6. c) The derived emission rate of ethylene together with the tracer mixing ratio (SF_6) as a function of time.

The same type of data as in Figure 4.3 but for position 2 are shown in Figure 4.4. The source/tracer ratio is different (32.5:1) than in position 1. It can be seen in Figure 4.4 (c) that the emission rate is fairly constant when the tracer is high and this indicates a

good measurement. The tracer weighted average over the whole shown period corresponds to 4.4 kg/h with a standard deviation of 20%.

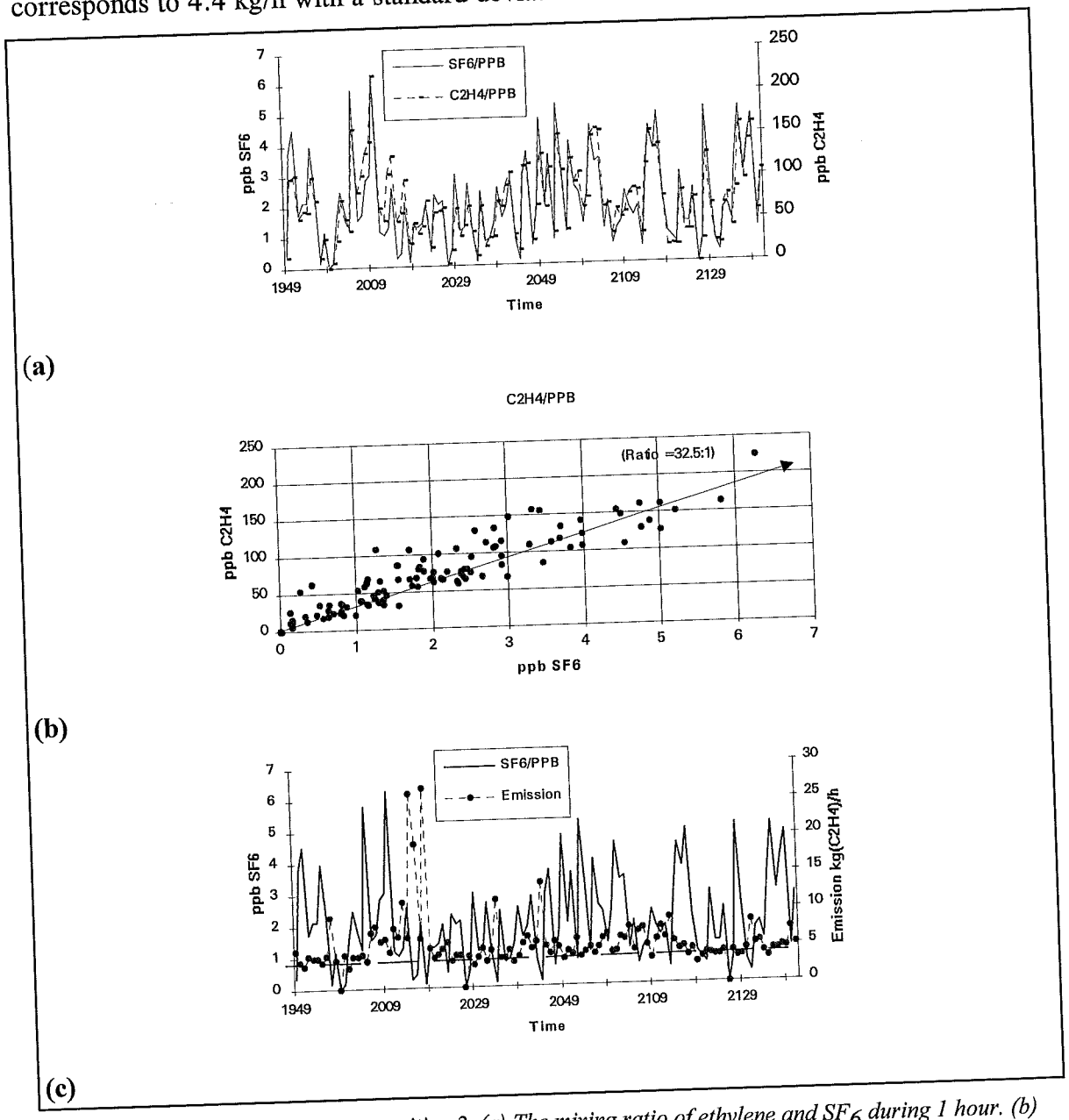

Figure 4.4. FTM measurements at position 2. (a) The mixing ratio of ethylene and SF_6 during 1 hour. (b) The mixing ratio of ethylene versus SF_6. (c) The derived emission rate of ethylene together with tracer mixing ratio (SF_6) over time.

In Figure 4.5 the measurements have been divided into 30 minute intervals and a separate tracer weighted average and standard deviation has then been calculated for each of those. The standard deviation is shown as error bars (±STD). It can be seen that the measured leakage rate at position 1 is approximately 2.8 kg/h while it is 60% larger at measurement position 2. This difference is probably caused by the fact that the measured plume at position 1 comes solely from the reactor. At position 2 a larger part of the EO plant will be measured since the tracer and source gases then will through a larger part of the plant. The obtained emission rate will therefore be larger.

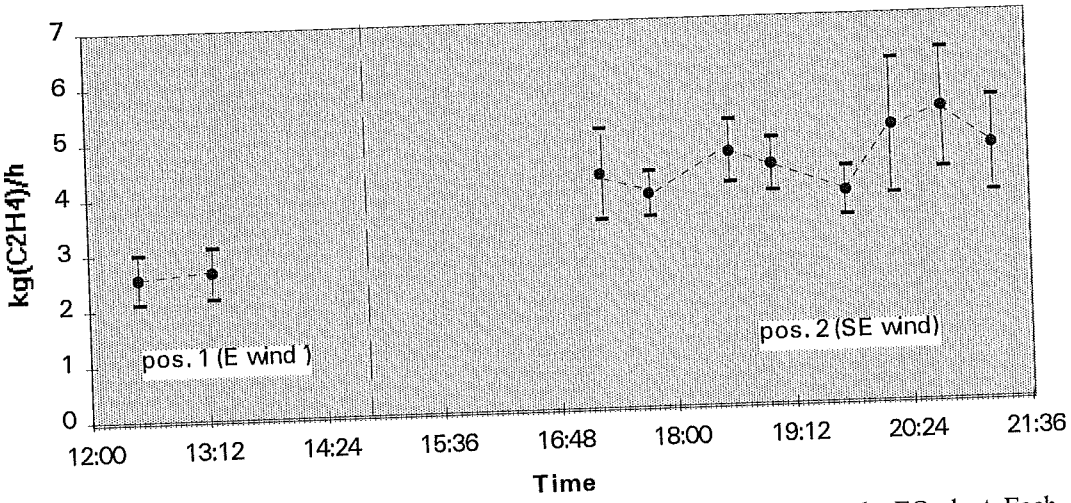

Figure 4.5. Measured emissions of ethylene on August 24 1994 from the reactor at the EO plant. Each value corresponds to a SF_6 weighted value measured over approx. 30 minutes. The measurements were performed at two locations. The error bars correspond to the SF_6 weighted standard deviation in the emission rates.

Another potential explanation for the difference in derived leakage rates between pos. 1 and pos. 2 is uncertainties in the source simulation by the tracer in the first position, due to a too short distance from the source. This may cause incomplete mixing between the tracer and source gas which may lead to errors in the mass flux obtained with the FTM. An underestimation of the mass flux will for instance be obtained from the FTM if a larger fraction of the tracer than of the source gas is measured. The main part of the tracer releases at the reactor were done at the ground level. If most of the leakages occur higher up and if the source and tracer gas do not mix entirely, then the leakage rate will be underestimated. Position 2 was placed considerably longer from the source than position 1 and even if the emissions of the tracer and source gas were located at different heights they would be able to mix better. Although this explanation is possible we believe that a bad source simulation would show larger variations in the measured tracer/source ratio than what is seen in the data in Figure 4.3.
A third possible explanation for the difference seen between pos. 1 and pos. 2 is that the actual emissions from the reactor change over the course of the day.

To summarize we believe that the measurements at pos. 2 were fairly good. In Figure 4.6 the wind direction at the measurement location together with the tracer weighted emission rates and their standard deviations are shown. It can be seen that the error bars are largest when the wind direction is most southerly. The error bars are smallest for wind directions below 125°. For these data points the source simulation by the tracer is rather good. This could be explained by the fact that when the wind is most easterly, the tracer and source gas travels through a larger part of the plant. The source and tracer gas will then be able to mix thoroughly and the ratio between the two species will thus become rather constant at the measurement location. It can be seen that despite the small error bars for the data with the most easterly winds the emission rates vary with ±10%.

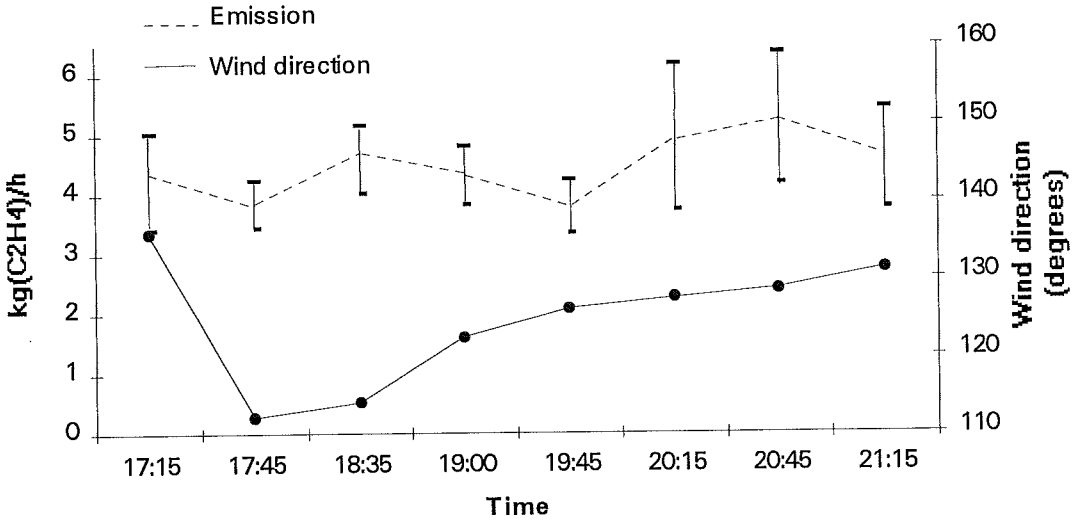

Figure 4.6. The average emission rates at position 2 over time. In addition the average wind speed and direction are shown.

4.2 The Akzo Nobel amine plant

In the amine plant ammonia and ethylene oxide react at high pressure and temperature in a reactor to form ethanol amines. These are later separated in a destillation process. The production of amines is approx. $4.8 \cdot 10^3$ kg/h. The main emittant is ammonia and the continuous leakage rate is estimated[3] to be less than 1.2 kg/h (10^4 kg/year). In addition there are point releases of up to $5 \cdot 10^3$ kg/year.

The main leakages are assumed to come from the reactor area. FTM measurements were performed there in the end of August 1994. Six tracer cylinders (SF_6) were distributed over the reactor area which have the approximate dimensions: height 20 m, base length 30 m and width 10 m. The measurement were performed 120 m southeast of the source, as shown in Figure 4.7.

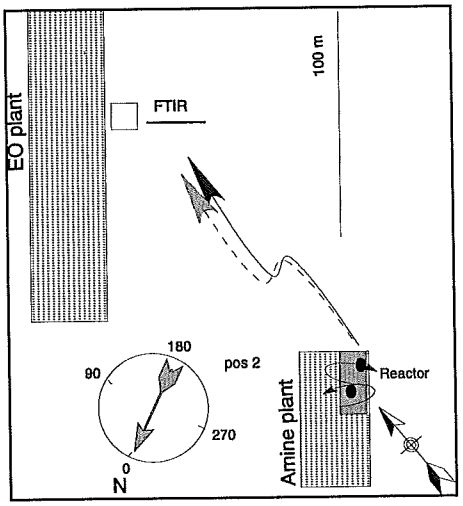

Figure 4.7. Schematic overview of the FTM measurements at the Akzo amine plant.

[3]Environmental report, 1994.

The FTM measurements were performed with the open 1 km White system described in section 2. During the later part of the measurements, maintenance work was performed in the reactor area.
In Figure 4.8 the Gaussian parameters for the plume are shown. The stability class during the measurements was neutral (D). This means that 95% of the plume mass at the ground level will be confined within 70 m.

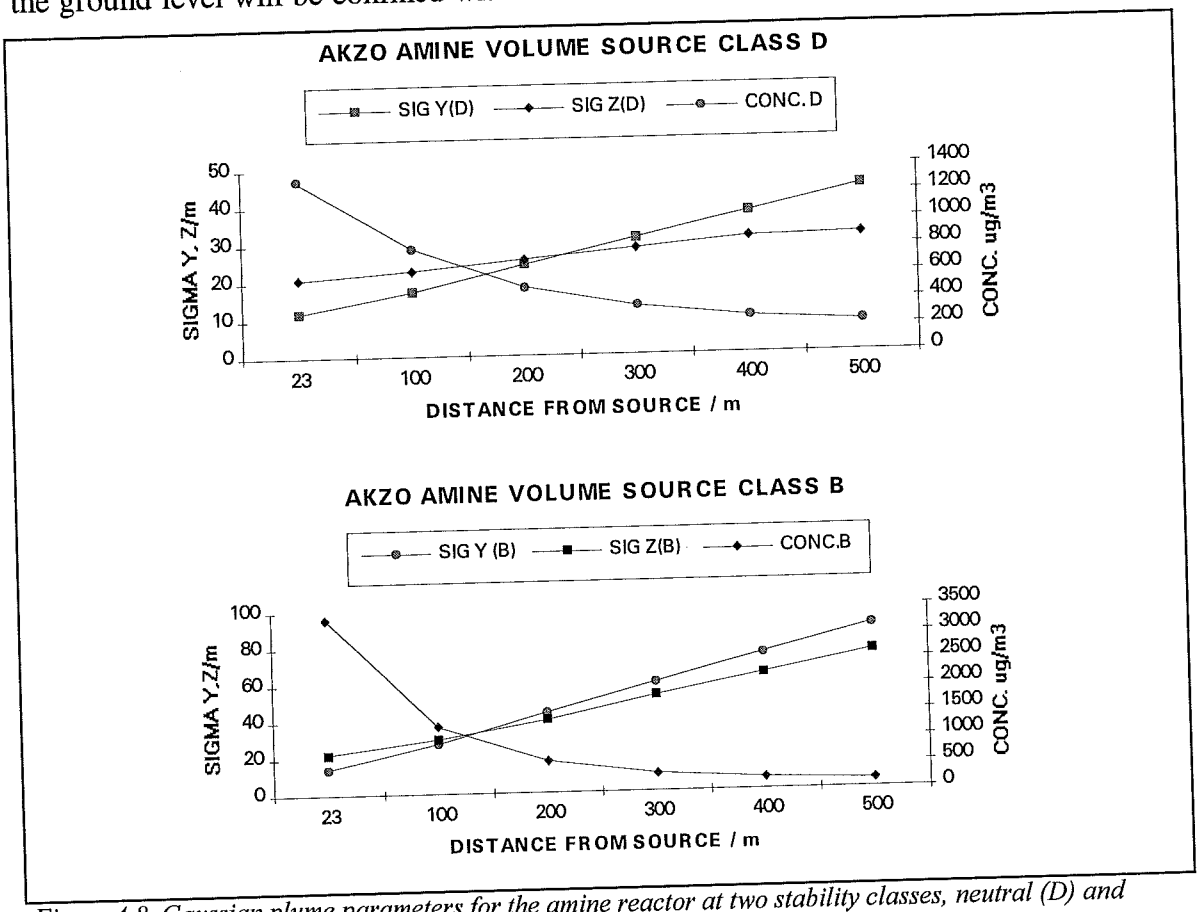

Figure 4.8. Gaussian plume parameters for the amine reactor at two stability classes, neutral (D) and unstable(B).

In Figure 4.9 results are shown from a FTM measurement of ammonia. The derived emission rate as well as the tracer mixing ratio (SF_6) are shown. It can be seen that the leakage rate is fairly constant during periods with high tracer mixing ratios. This indicates a good source simulation. The tracer weighted average is 1.1 kg(NH_3)/h with a standard deviation of 28%. In Figure 4.10 a measured spectrum of ammonia is shown together with a fitted spectrum. In addition the difference between the two spectra (residual) is also shown

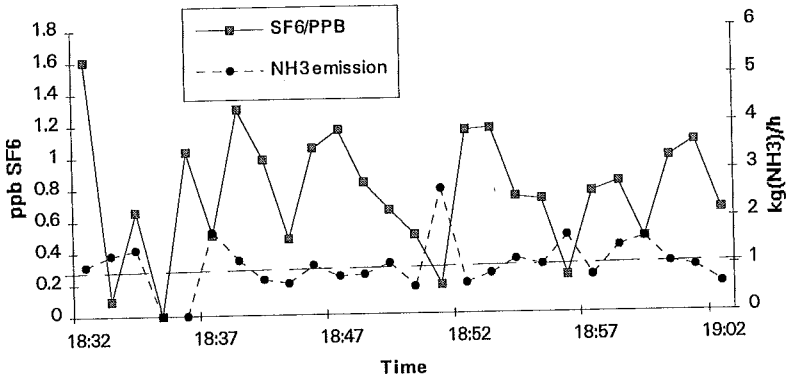

Figure 4.9. The derived emission rate of NH_3 from the Akzo Nobel amine plant together with the tracer mixing ratio (SF_6) over time.

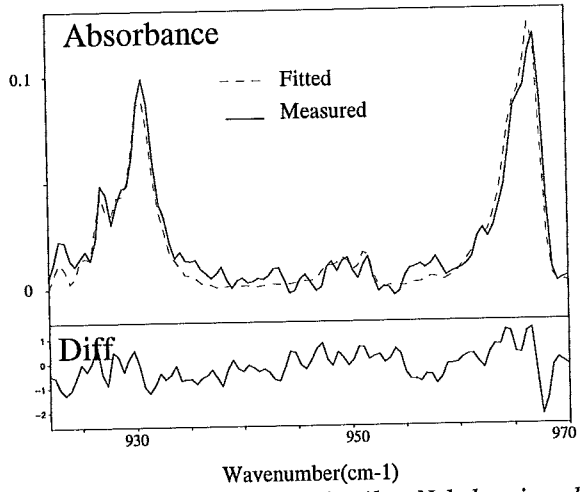

Figure 4.10. Measured ammonia spectrum leeward of the Akzo Nobel amine plant, corresponding to 102 µg/m3. In addition a fitted spectrum and the difference between the two spectra are shown.

As mentioned earlier, maintenance work was performed in the amine plant during part of the measurements. In Figure 4.11 the tracer mixing ratio and the derived emission rates of ammonia are shown during the maintenance period. It can be seen that there is a large increase in the emission rates from 1 to 65 kg/h around 19:40.

In the FTM technique the stability of the derived emission rates is used as a quality parameter for a good source simulation by the tracer. Since the ammonia emissions vary over time in the data in Figure 4.11 there is no way to tell whether the quality of the source simulation by the tracer is good or not. It was on the other hand shown in Figure 4.9 that the tracer simulated the source well during normal operation of the plant. Under the assumption that the ammonia leakages during the maintenance work originate from the same region as during the normal operation, it can therefore be assumed that the derived ammonia emission rates are fairly correct when the tracer mixing ratio is high (>0.5 ppb). In conclusion the data in Figure 4.11 illustrates well how time variations in the emission rates can be measured, even though these measurement are connected with large potential errors.

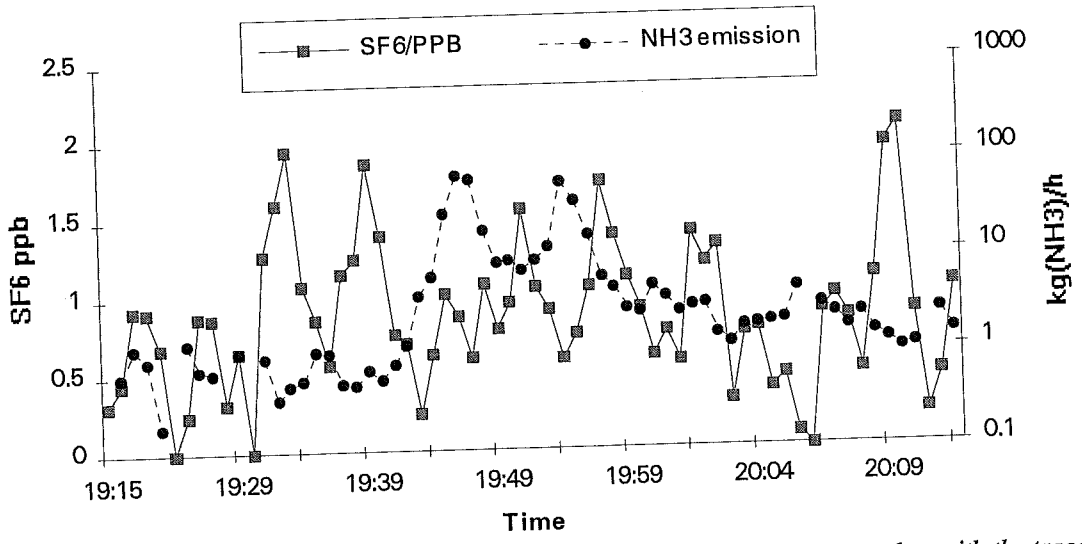

Figure 4.11. The derived emission rate of NH_3 from the Akzo Nobel amine plant together with the tracer mixing ratio (SF_6) over time. The measurements were performed during maintenance work. (Note the logarithmic scale on the NH_3 emission).

4.3 The Borealis Cracker plant

At the Borealis Cracker plant the main products are ethylene and propylene. These compounds are produced from the raw materials naphtha, ethane, propane and butane by heating in cracker furnaces. The raw compounds dissociate to unsaturated hydrocarbons such as ethylene, propylene, butene, butadiene. In addition one also obtain aromatic distillates, fuel gas, and heavier compounds. A part of the butene and butadiene is further refined to MTBE. The production of ethylene and propylene 1994 was approx. $45 \cdot 10^3$ kg/h and $21 \cdot 10^3$ kg/h, respectively. The main emittants are ethylene and propylene and the emissions of these compounds are frequently measured by the conventional SF_6 method as described in section 2. The measurements are conducted by the process laboratory at the cracker plant and show a steady decrease in the leakage rates of VOCs over the last decade from 223 kg/h in 1985 to 92 kg/h in 1994[4].

The main leakages at the Borealis cracker plant are believed to originate from the process area with the approximate dimensions: 70 m width, 60 m base width and 5 m height. In Figure 4.12 a schematic drawing of the process area is shown together with three optical paths that have been used for FTM measurements. In addition typical release points of the SF_6 inside the process area are shown together with measurement points for the conventional SF_6 method.

Several measurement paths are shown in Figure 4.12. Path 1 and 2 correspond to 106 and 212 m and they were used in May 1995 for FTM measurements utilizing the Long Path system. The distance from the source was here 160 m. Path 3 was used in April 1993 with the 1 km White system at a distance of 80 m from the source.

---

[4]Environmental report, 1994.

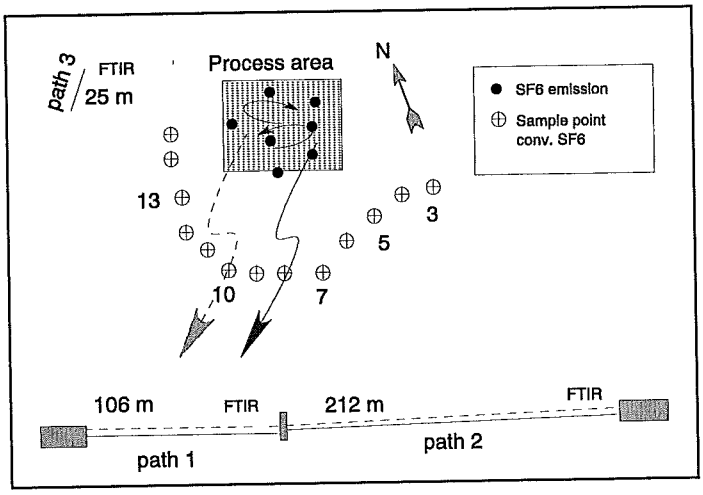

Figure 4.12. Schematic overview of the FTM measurements at the Borealis cracker plant. SF_6 release points are shown as well as locations for the conventional SF_6 measurements.

In Figure 4.13 Gaussian parameters for the leakages from the process area are shown. It can be seen that the cross section of the plume is fairly large at distance of 150 m (95% of the plume mass will be confined within 300-400 m).

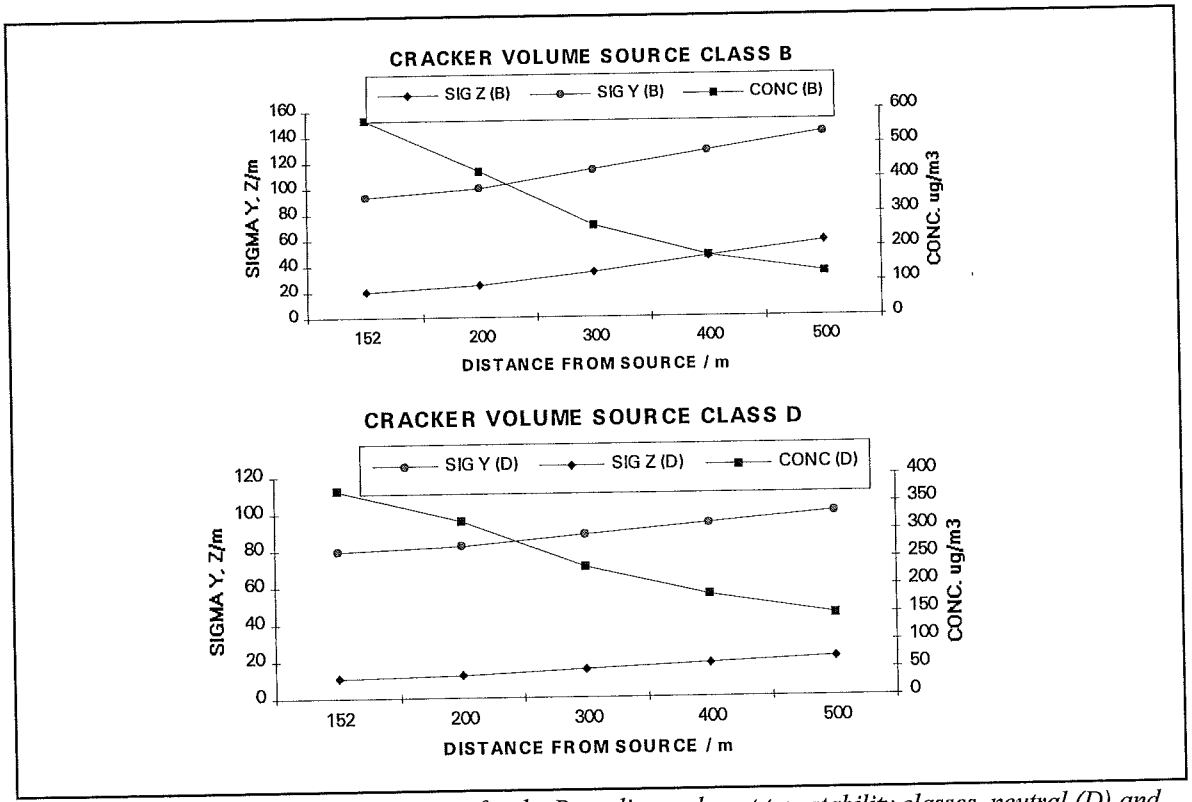

Figure 4.13. Gaussian plume parameters for the Borealis cracker at two stability classes, neutral (D) and unstable(B).

In the spring of 1993 FTM measurement were conducted at path 3 with the White system as shown in Figure 4.13. This was an initial test and the flow rate of SF_6 was varied quite a lot. The winds were easterly with low to moderate wind speeds and overcast. In Figure 4.14 the measured mixing ratios of SF_6 and ethylene are shown. The derived emission rate together with the tracer mixing ratio is shown in Figure 4.15. The tracer weighted average over the shown period is here 32 kg/h with a

standard deviation of 12%. In these measurements there were uncertainties about the release rate (±15%) and the evaluation of the ethylene and SF_6 was conducted in a more crude way then what has been done for the rest of the data in this study.

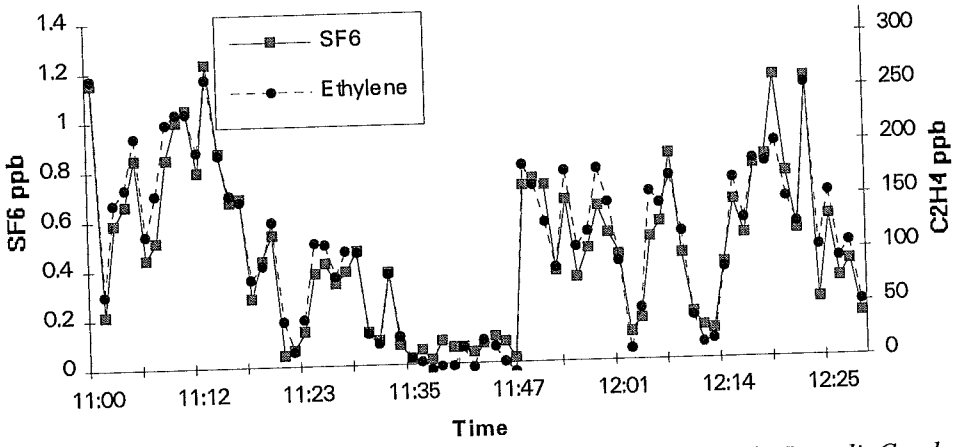

Figure 4.14. Mixing ratios of the tracer (SF_6) and source gas (C_2H_4) at the Borealis Cracker.

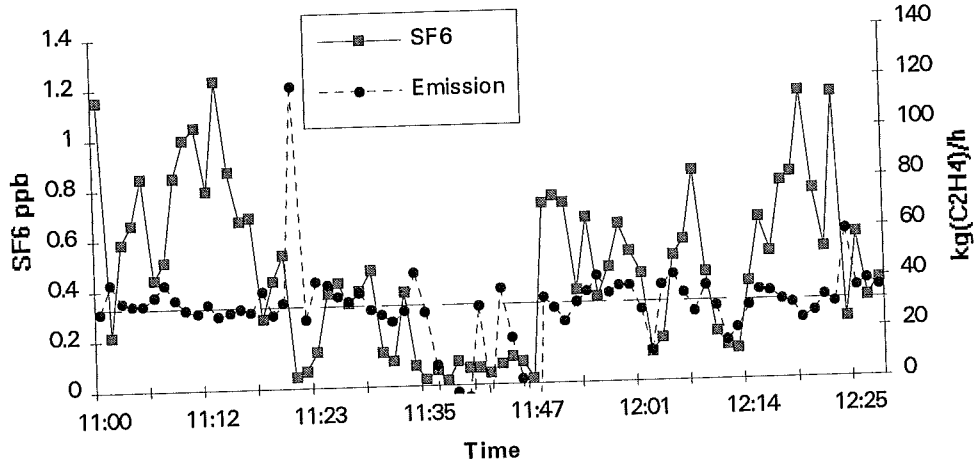

Figure 4.15. Mixing ratio of SF_6 and emission rate of C_2H_4 at path 3 in April 1993.

In Figure 4.16 mixing ratio measurements of ethylene, propylene and SF_6 are shown which were conducted along path 1 on May 12, 1995. The wind was northwesterly with moderate speeds (6 m/s) and clear sky .
The two measured source gases have been plotted versus the tracer in Figure 4.17. It can be seen that the ethylene/SF_6 ratio is approx. (40:1) while it is lower for the propylene/SF_6 ratio (23:1). In Figure 4.18 and 4.19 the derived emissions of the two source gases are shown together with the tracer mixing ratio. It can be seen that the emission rate of ethylene is fairly constant when the tracer mixing ratio is high and this indicates a good source simulation. The tracer weighted average emissions for ethylene was 15.1 kg/h with a standard deviation of 19%. The derived emission rates for propylene varies more than for the ethylene and this may be due to noise in the spectral evaluation but also caused by a worse source simulation. The tracer weighted average for the propylene is 13 kg/h with a standard deviation of 25%.

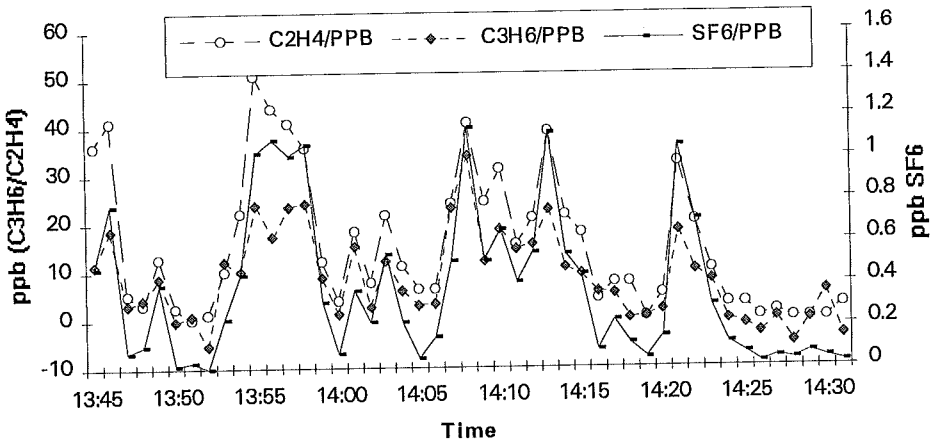

Figure 4.16. Measurements of ethylene, propylene and SF_6 at the Borealis cracker plant.

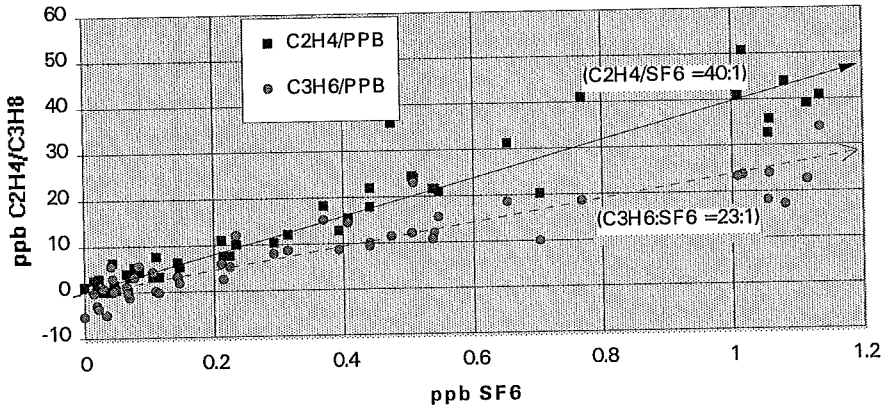

Figure 4.17. *The mixing ratio of ethylene and propylene versus SF_6.*

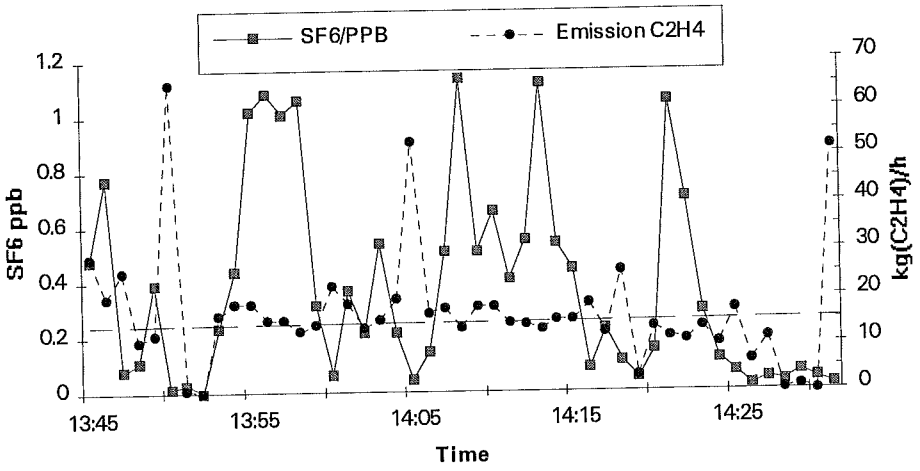

Figure 4.18. Measured mixing ratio of SF_6 and emission rate of C_2H_4.

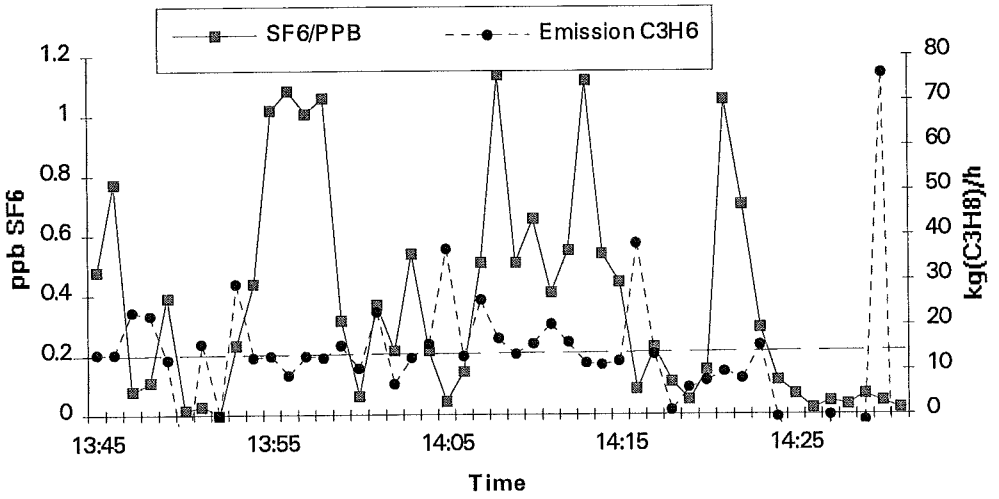

Figure 4.19. Measured mixing ratio of SF_6 and emission rate of C_3H_6.

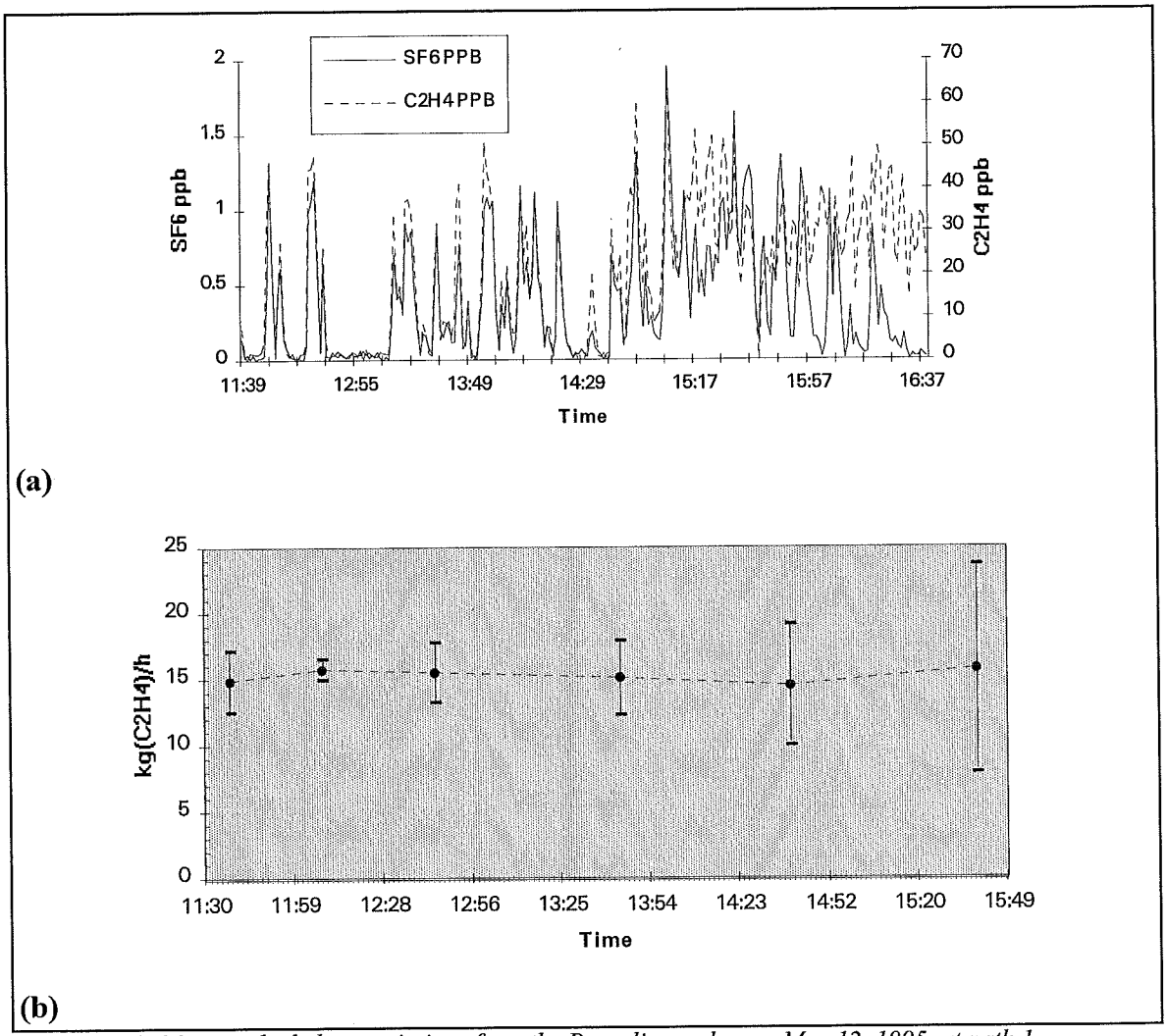

Figure 4.20. Measured ethylene emissions from the Borealis cracker on May 12, 1995, at path 1. (a). Mixing ratios of the source and tracer gases. (b) Tracer weighted averages over 15-60 data point over 0.25-1 hour. In addition the weighted standard deviations in the emissions rates for each interval are shown as error bars, indicating the quality of the source simulation.

In Figure 4.20 the FTM measurements of ethylene along path 1 have been divided into 30 minute intervals and a separate SF_6 weighted average has then been calculated for each of those intervals. The larger error bars in the FTM measurement in the end of the day are caused by the wind shifting to the west. The individual emission-values differ up to 4% from the total tracer weighted average of 15 kg/h. The standard deviation is 21% which indicates a good source simulation by the tracer.

4.3.1 Comparison between the FTM and the conventional SF_6 method

In Figure 4.21 FTM measurements along path 2 on May 9, 1995 are shown. The mixing ratio of SF_6 and emission rate of ethylene are displayed versus time, yielding a tracer weighted average emission rate of 13 kg/h with a standard deviation of 17%. Earlier on the same day measurements were conducted with the conventional SF_6 method. Ethylene, propylene and SF_6 were here analyzed at 15 locations leeward of the process area, as illustrated in Figure 4.12. This was done by sampling air into plastic bags placed at the 15 locations over a 30 minute period. The bags were later analyzed by gas chromatography.
In Figure 4.22 the results from the conventional point measurements are shown. Leakage rates of 11.8± 1.5 kg/h of ethylene and 9 kg/h of propylene were obtained. It can be seen in the figure that at points no. 1 to 4 (the most easterly ones) the correlation between the source and tracer gas was quite bad. This was caused by the existence of other sources which were not simulated by the tracer releases. From the results in Figure 4.22 it can be deduced that the LPFTIR measurements along path 2 correspond to the gas mixing ratios measured at point 5 to point 9. The correlation between the tracer and source gas was fairly good over these points according to the results in Figure 4.22, indicating that the ethylene measured over these points is well simulated by the tracer gas.

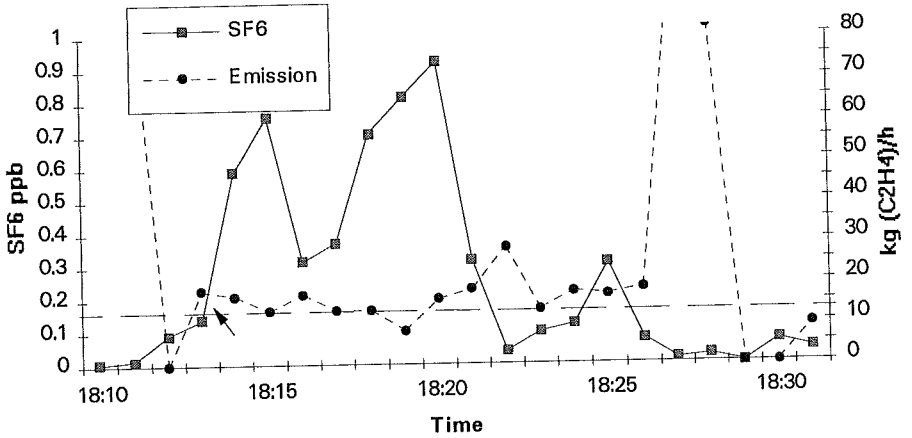

Figure 4.21. Measured mixing ratio of SF_6 and emission rate of C_2H_4.

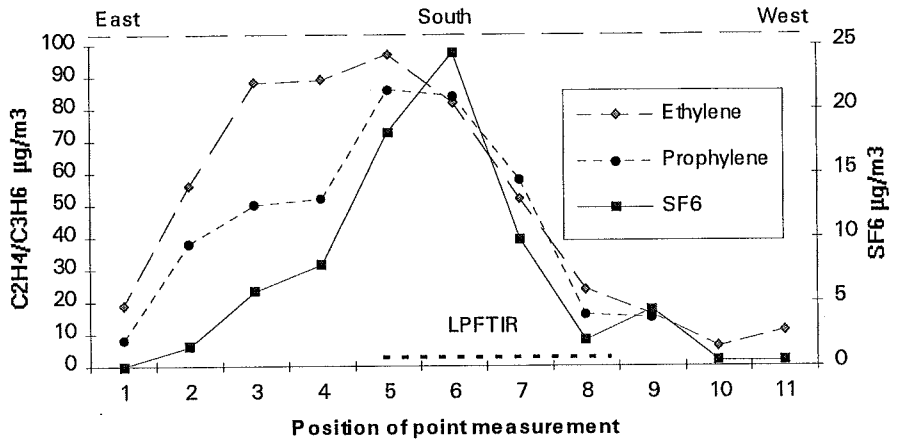

Figure 4.22. Conventional measurement of SF_6 ethylene and propylene in 11 positions covering east to west. The part of the plume covered by the LPFTIR measurements at path 2 is also shown.

In Figure 4.23 the measurements at the Borealis cracker plant have been summarized. The measurements performed by the process laboratory in 1993 and 1995 are shown (white diamonds) as well as our FTM measurements (black circles) in April 1993 and May 1995. It can be seen that the emissions have decreased substantially over the time period shown. It can also be seen that there are considerable variations (up to 40%) in the emissions. There are several reasons for this behavior including measurement errors and variations in the emissions due to varying wind speed, wind direction and temperature. It can be seen that the results of the FTM are within the variability of the values from the conventional SF_6 method.

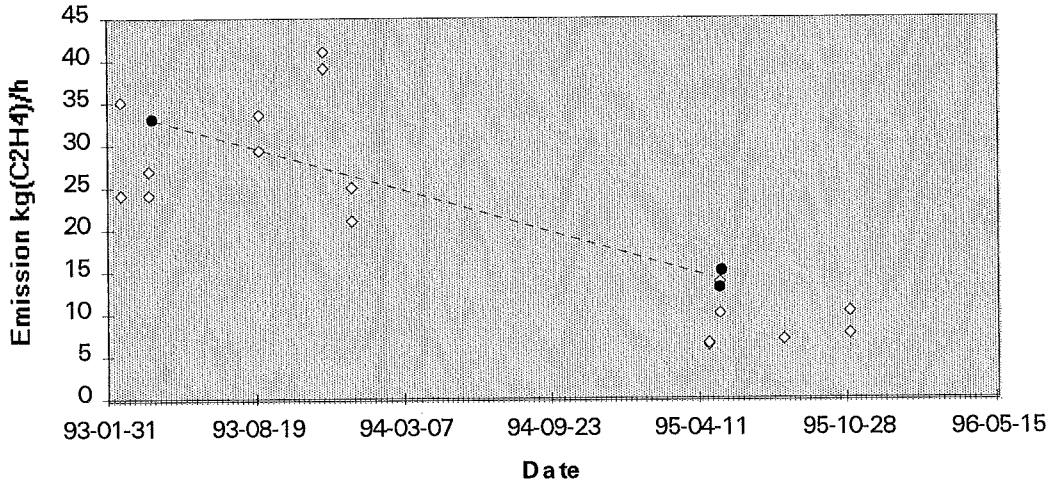

Figure 4.23. Measured mass fluxes at the Borealis Cracker plant. A comparison of the results obtained from the conventional SF_6 method (white diamonds) and the FTM (black circles).

4.4 The high pressure plant at Borealis polyethylene.

At the high pressure plant polyethylene is produced from ethylene and other additives. This is done in three stages: gas cleaning, reactors and further processing. The ethylene is first condensed by compression to 35 bar. After cooling to -30°C and a pressure increase to 100 bar the ethylene is pumped to the reactor were the pressure is increased to 2.3 kbar. In the reactor stage the ethylene is polymerized to polyethylene at 300°C. The unreacted ethylene is returned back to the gas cleaning stage where it is cooled, condensed and purified in destillation columns and then returned to the reactor again. The approximate dimensions of the gas purification stage are: height 10 m, width 45 m and length 15 m. For the reactor area the dimensions are: height 10 m, width 50 m and length 50 m. At the gas purification stage there are cooling fans which blow the air upwards.

FTM measurements were performed leeward of the Borealis polyethylene plant at two positions at a distance of 270 m and 300 m from the gas purification stage, as shown in Figure 4.24. The single ended long path system in section 2.1.3 was used for all measurements. The tracer gas (SF_6) was released at 6 locations, 3 at ground level and 3 at 10 m height, in the vicinity of large fans which raised the air upwards. The release rate of SF_6 in each location was approx. 0.2 kg/h. There was overcast conditions and the wind speed was 3-5 m/s.

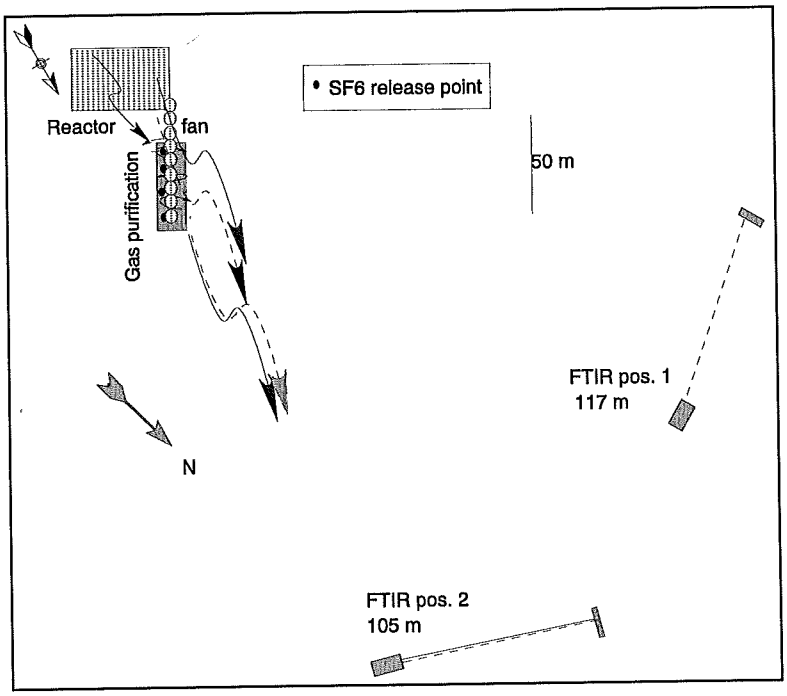

Figure 4.24. Schematic overview of the FTM measurements from the gas purification stage at the Borealis low pressure plant. The locations for the tracer releases are shown.

In Figure 4.25 the Gaussian plume parameters are shown for the high pressure plant. It can be seen that at the distance of 300 m 95% of the plume mass at the ground level will be confined within 250-350 m, depending on the stability class.

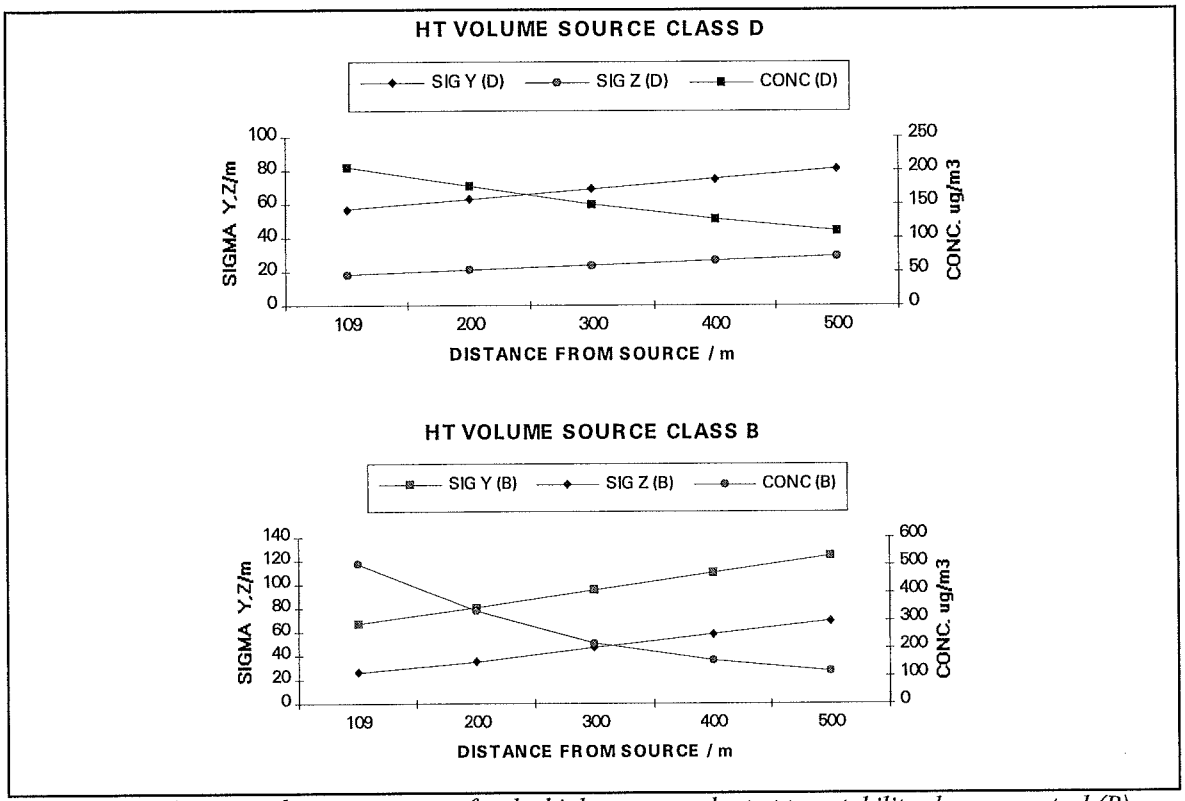

Figure 4.25. Gaussian plume parameters for the high pressure plant at two stability classes, neutral (B) and unstable(D).

In Figure 4.26 (a) the mixing ratio of the tracer (SF_6) and the source gas (C_2H_4) are shown, from the gas purification stage and reactor at the Borealis high pressure plant. The measurements were performed at pos. 2 on June 16, 1995. Three different time resolutions were used (60, 30 and 10 s) and the time periods during which these were used are indicated in the figure. In Figure 4.26 (b) the source gas mixing ratio is shown versus the tracer mixing ratio. A correlation between the two gases can be seen. Below a SF_6 mixing ratio of 0.2 ppb the correlation seem to become quite bad however.

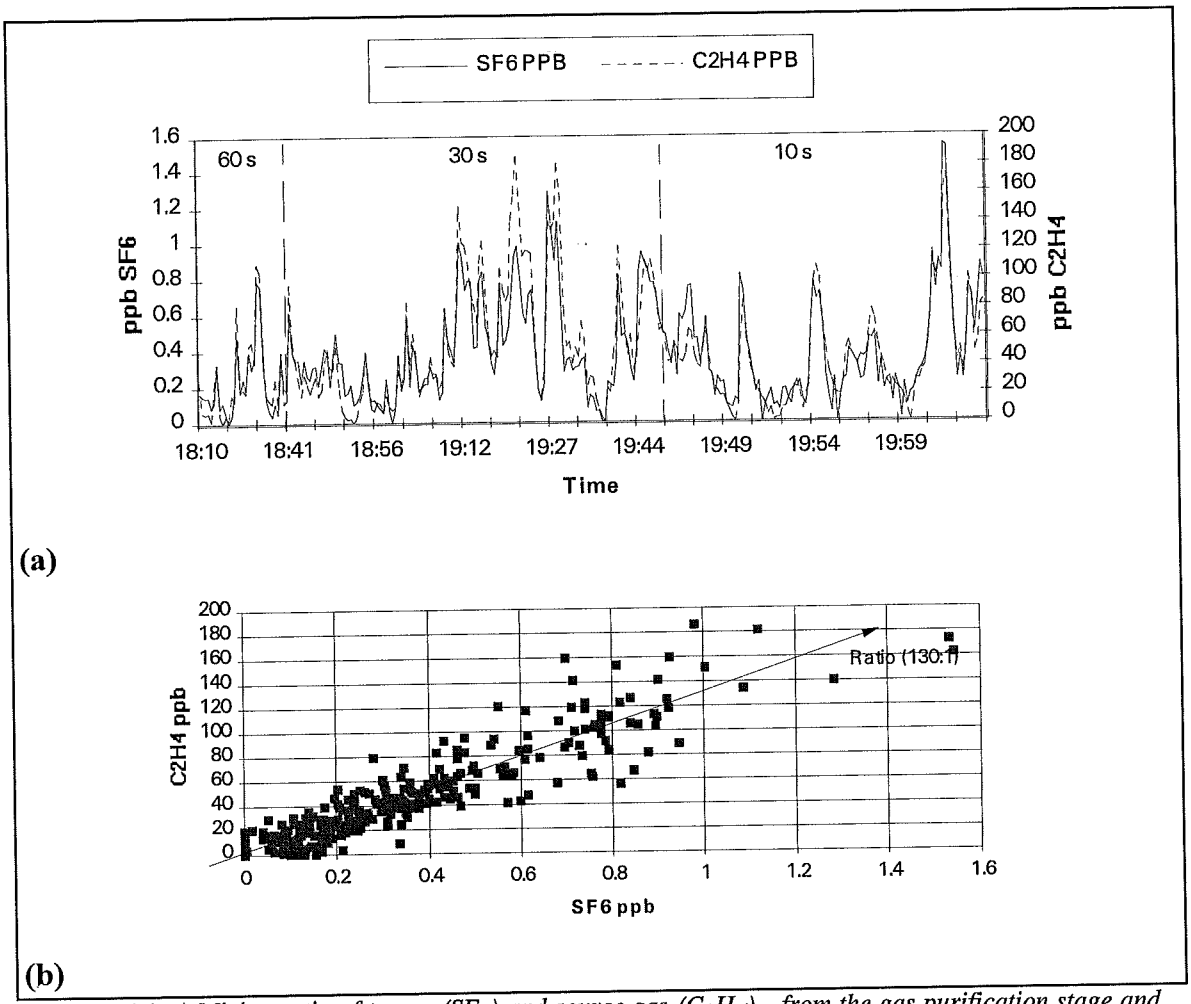

Figure 4.26. a) Mixing ratio of tracer (SF_6) and source gas (C_2H_4) , from the gas purification stage and reactor at the Borealis high pressure plant. The measurements were performed at pos. 2 on June 16 1995. Three different time resolutions were used, 60, 30 and 10 s and these periods are indicated.
b) Mixing ratio of ethylene plotted versus tracer (SF_6).

In Figure 4.27 (a) the mixing ratios of SF_6 and ethylene as a function of time are shown at pos. 2, measured on June 15, 1995. Here we tried to conduct measurements at high time resolution 10s/spectrum. In Figure 4.27 (b) the tracer and derived emission rate is shown. One can see that the ratio is quite constant during periods with high tracer values which indicates an excellent source simulation. The tracer weighted average emission is here 28.0 kg(C_2H_4)/h with a standard deviation of 14%.

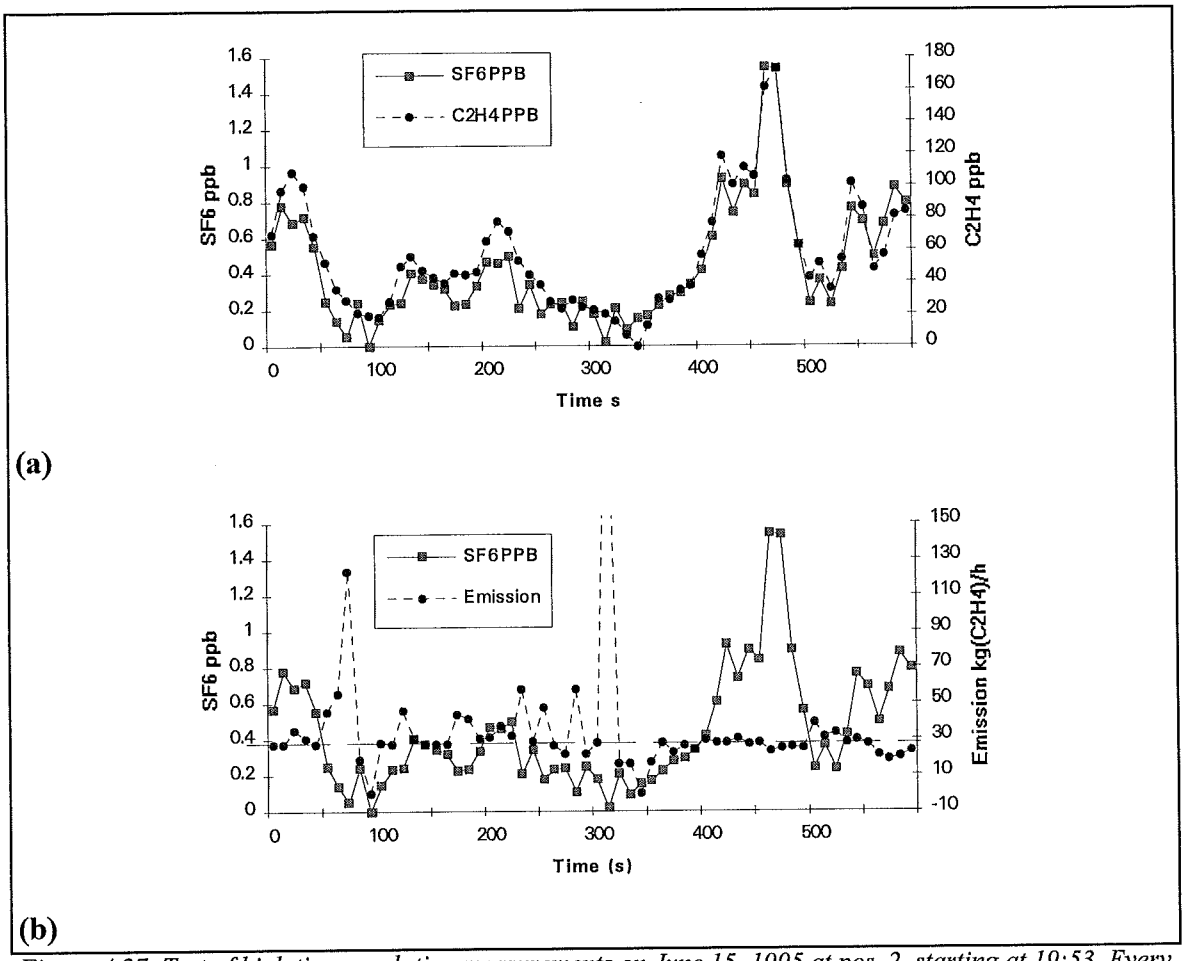

Figure 4.27. Test of high time resolution measurements on June 15, 1995 at pos. 2, starting at 19:53. Every point corresponds to 2 coadded spectra measured over 10 s. a) The mixing ratio of the tracer (SF_6) and source gas (ethylene) versus times. (b) Mixing ratio of the tracer and derived emission rates of ethylene.

In Figure 4.28 a measured absorbance spectrum is shown corresponding to the value around 480 s in Figure 4.27 (a). The broad absorbance corresponds to SF_6 and the sharp to ethylene (see Figure 3.1). In addition a fitted synthetic spectrum is shown containing 1.6 ppb SF_6 and 180 ppb ethylene. The noise level in the spectrum in Figure 4.27 is around 10^{-3} absorbance units, for a total optical pathlength of 210 m. This implies a detection limit for ethylene of 3 ppb. This should be compared to the detection limit for a time resolution of 60 s/spectrum which is a factor of two better.

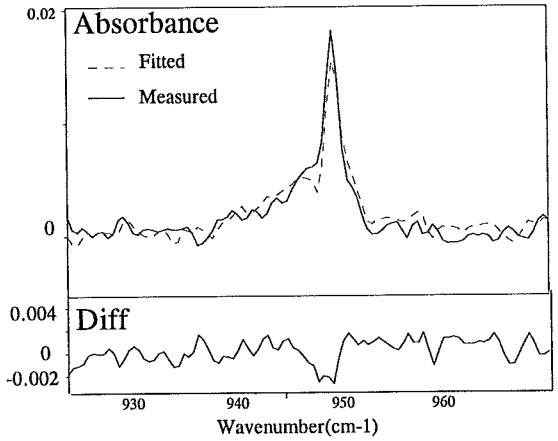

Figure 4.28. Measured absorbance spectra of SF_6 (broad structure) and ethylene (sharp) corresponding to 2 coadded spectra over 10 s. In addition a fitted synthetic spectrum and the difference is shown.

In Figure 4.29 a fraction of the data from Figure 4.28 is shown measured at 19:15. The derived emission rates of ethylene are shown together with the tracer mixing ratio. The SF_6 weighted average was here 34 kg/h with a standard deviation of 22%.

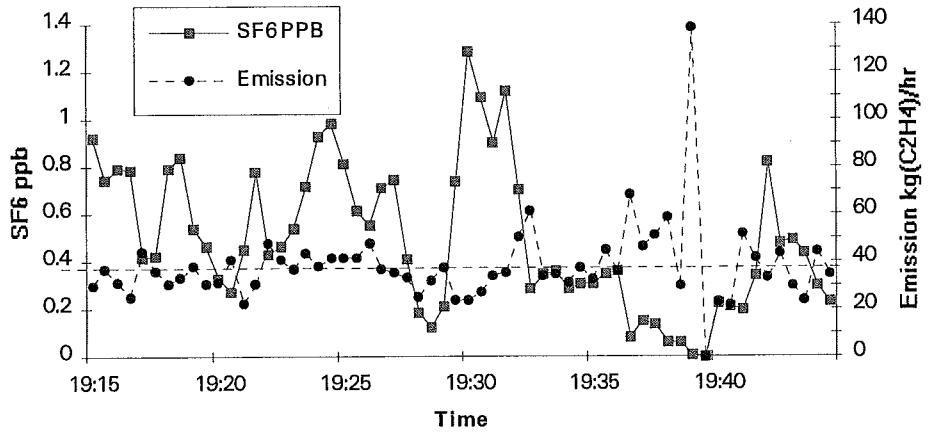

Figure 4.29. Mixing ratios of the tracer (SF_6) and derived leakage rates from the reactor and the gas purification stage at the Borealis high pressure plant. The time resolution used was 30 s/spectrum.

In Figure 4.30 the FTM measurements of ethylene from the gas purification stage and reactor at the high pressure plant are summarized. Each value corresponds to a weighted average over 30-60 data points. The error bars correspond to the standard deviation (±STD) in the emission rates over each averaging period.
The data in Figure 4.30 were measured both in pos. 1 and pos. 2 as was illustrated in Figure 4.24. The time resolution used was different over the measurement period. The first four data points corresponds to a used time resolution of 60 s per spectrum. The two following ones correspond to a time resolution of 30 s/spectrum and the last three points correspond to a time resolution of 10 s/spectrum. It can be seen that the time resolution seem to affect neither the absolute value of the emission rate nor the error bars.

The FTM measurements at pos. 1 had bad quality, as can be seen in the error bars in Figure 4.30, and we believe the poor quality was caused by influence of the two low pressure plants at the Borealis polyethylene production site. This influx also increased the derived emission rate.
The FTM measurements at pos. 2 were quite good however, and in this case the winds were such that all emitted ethylene had to come from the high pressure plant (reactors or gas purification stage). It can be seen that the individual values at pos. 2 differ up to 16% from the total average of 32 kg/h. These variations can be caused by either variations in the leakage rates or by measurement artifacts.

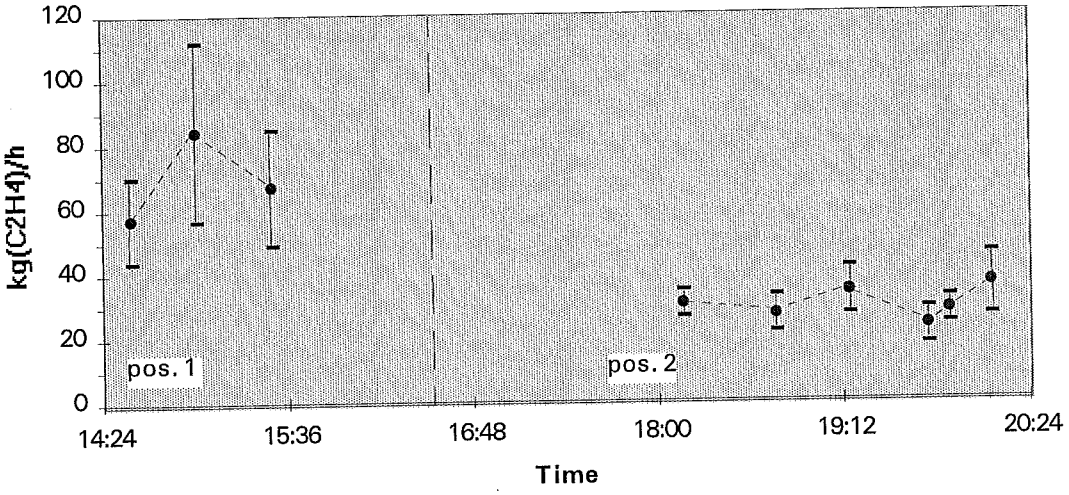

Figure 4.30. Measured ethylene emissions from the Borealis polyethylene plant on June 15, 1995. Each value corresponds to a weighted average over 30-60 data points. The error bars correspond to the weighted standard deviations (STD) in the emissions rates. At pos. 1 a large part of the emissions from the whole polyethylene production site blows into the measurement path while at pos. 2 only the emissions from the reactor and gas purification stage at the high pressure plant blows into our measurement path.

4.5 The low pressure plant at Borealis polyethylene

In the low pressure plant polyethylene is produced from ethylene and other additives. Instead of performing the polymerization at high pressure in a reactor, in the way that was described in the previous section, it is performed in a fluidized bed containing metallic catalysts on Silica gel. The catalysts are extremely sensitive to impurities in the feedstock and therefore the latter are purified in a purification stage. After the gas purification stage the raw compounds (ethylene, butene) are taken to a circulation system where they are mixed with the catalyst. The mixture is further taken to the reactor where polymerization of the ethylene occurs at approx. 21 bar and a maximum temperature of 110°C. Unreacted gas is taken back to the circulation system. The approximate dimensions of the low pressure plant are: height 25 m, width 30 m and length 40 m. For the gas purification they are: height 5 m, width 20 m and length 40 m. The average production in the plant[5] is approximately $15 \cdot 10^3$ kg/h and the emissions of ethylene (which is the main emittant) are estimated to be approx. 5 kg/h.

FTM measurements were conducted at the low pressure plant no. 2 at the Borealis polyethylene on September 8, 1994. The 1 km White system was used in the location shown in Figure 4.31. Due to maintenance work only one out of two reactors was operating during the measurements. We first tried to perform FTM measurements on the reactor area. Evidence for another stronger source, the gas purification stage, was directly seen and this source disturbed the measurements. The tracer release was thereafter moved from the reactor area to the gas purification stage and these results are shown in Figure 4.32. The measurements were performed at a distance of 110 m. The wind was SE-E with low-moderate wind speeds and overcast. The tracer (SF_6) was released from 4 bottles placed at ground level with a total release rate of 0.5 kg/h.

In Figure 4.32 (a) the mixing ratio of the measured ethylene is shown versus the tracer. In Figure 4.32 (b) the derived emission rate is shown together with the tracer. It can be seen that the emissions are fairly constant when the tracer mixing ratio is high and this indicates a good source simulation by the tracer. A weighted average of 3.1 kg/h is obtained with a standard deviation of 30%.

---

[5]Environmental report, 1994

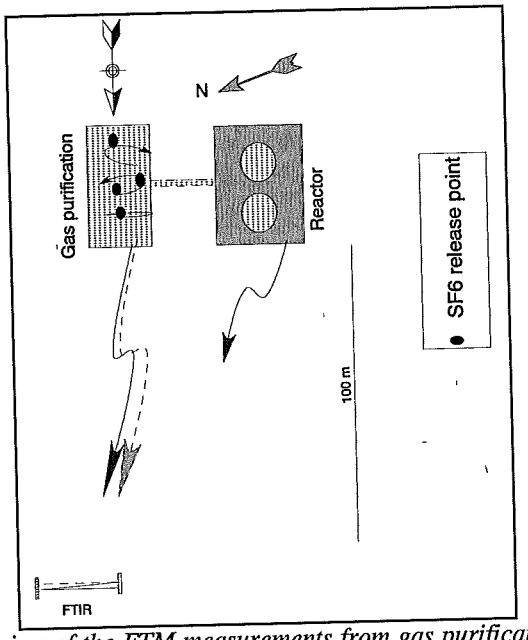

Figure 4.31. Schematic overview of the FTM measurements from gas purification stage at the Borealis low pressure plant. Locations for the tracer releases are shown.

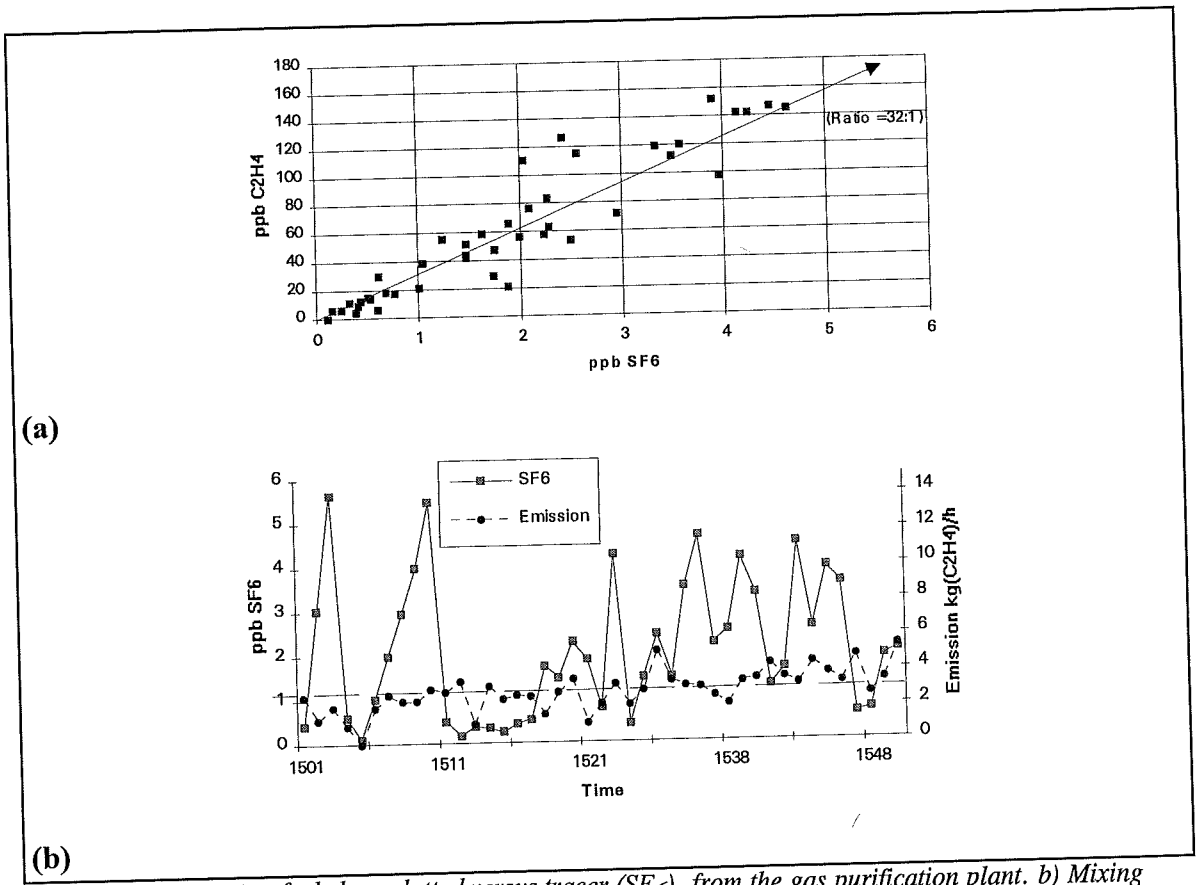

4.32. a) Mixing ratio of ethylene plotted versus tracer (SF_6), from the gas purification plant. b) Mixing ratio of the tracer (SF_6) and derived leakage rate.

In Figure 4.33 (a) the FTM measurements of ethylene from the gas purification stage have been divided into 30 minute intervals and a separate tracer weighted average emission and standard deviation has then been calculated for each of those intervals. The individual values differ up to 16% from the total average of 3.1 kg/h. These

variations can be caused by either variations in the leakage rates or by measurement artifacts. The direction of the wind and ground speed are shown in Figure 4.33 (b). It can be seen that the errors bars in the emission are largest when the wind is most easterly.

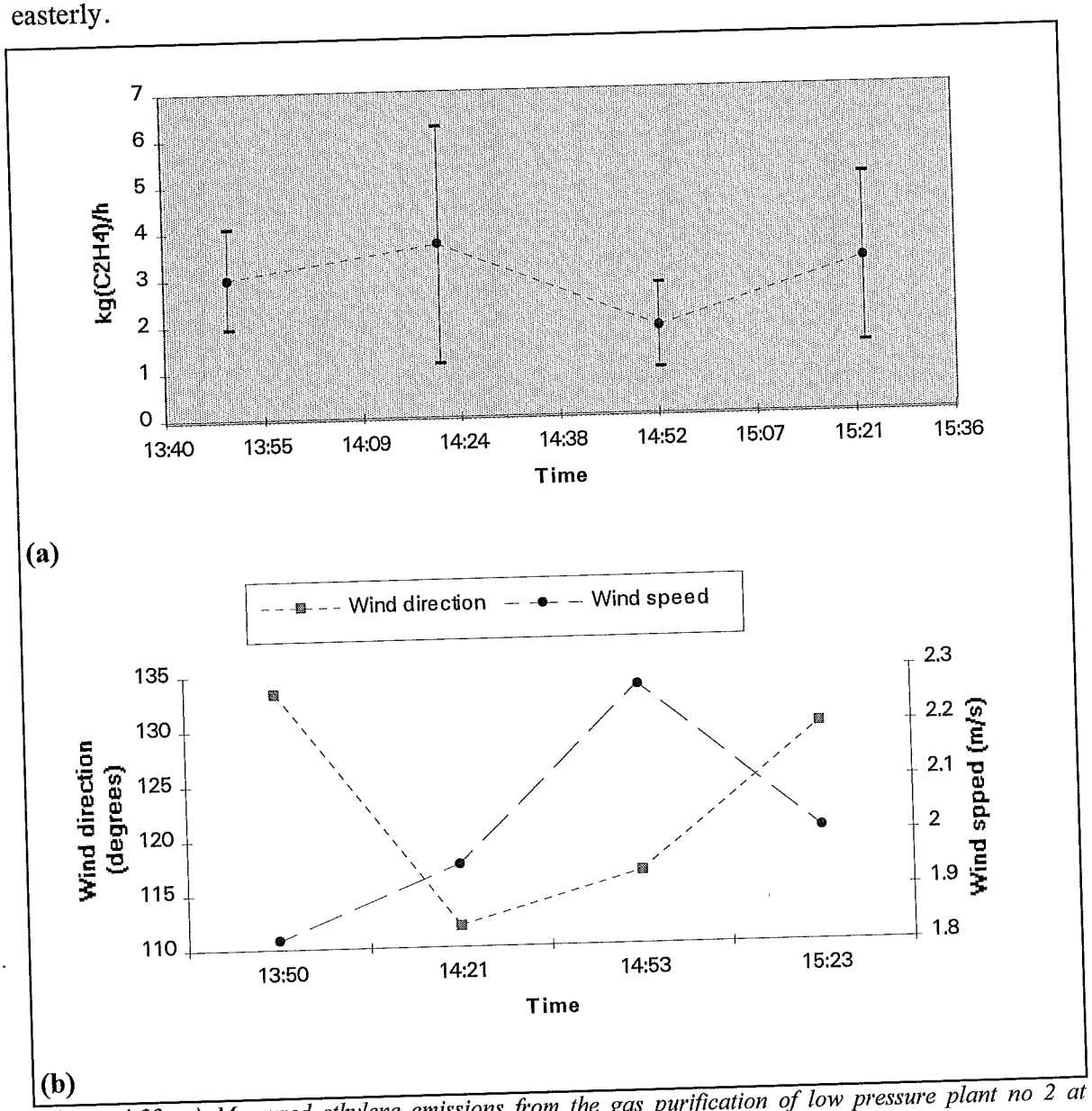

Figure 4.33. a) Measured ethylene emissions from the gas purification of low pressure plant no 2 at Borealis polyethylene on September 8, 1994. Each value corresponds to a weighted average over a time period of 30 min -1 hour. The standard deviation in the emission rates for each interval are shown with the error bars (± STD).
b) The wind direction and wind speed at the ground at the measurement location are shown.

4.6 Refinery

During the summer of 1994 several long path measurements were performed at the Scanraff Refinery in Lysekil. The main purpose of these measurements was to determine the hydrocarbon emissions from several crude oil tanks (1402-1 and 1401-1) located on the southwest part of the plant. The approximate dimensions of the tanks are 25 m in height and 50 m in diameter. The tanks are equipped with a floating roof and the height of the roof is dependent on the amount of oil in the tank, which typically follows a 28 hour cycle. The main emissions from the tanks are believed to originate from leakages along the seal between the tank wall and roof, as illustrated in Figure 4.34 (a). The cavity above the tank roof will then slowly become filled with vapors. Once in a while the wind will blow into the cavity and create outburst of hydrocarbons. A fraction of these hydrocarbons will blow into the wake, leeward of the tank.

Several tracer gases were released during the experiments in order to assist in estimating the hydrocarbon release rates. Tracer gas lines were lowered into the tank and on the leeward side of the tanks. Two tracers species were used: N_2O and CO. The first species was emitted from the middle of the floating roof while the latter was emitted on the top of the tank on the leeward side (grey arrows). Measurements were performed at a distance of 120 m from the tank with the open 1 km White system as shown in Figure 4.34 (b).

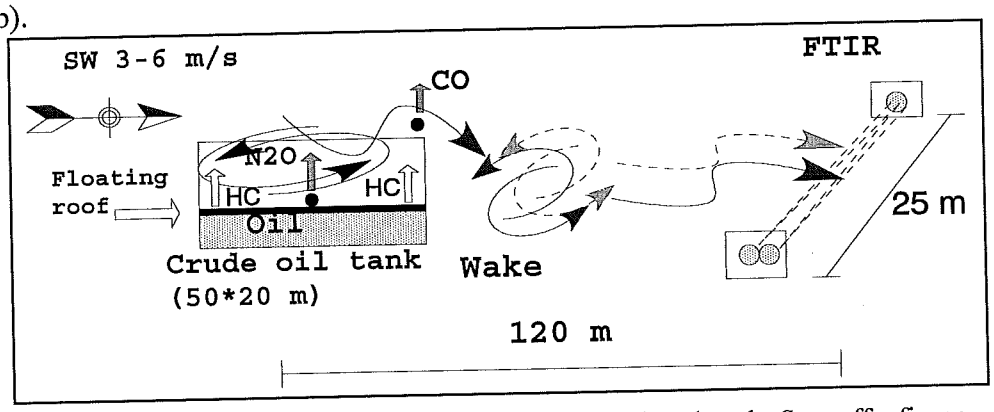

Figure 4.34. a) Schematic overview of the measurements in the tank park at the Scanraff refinery.

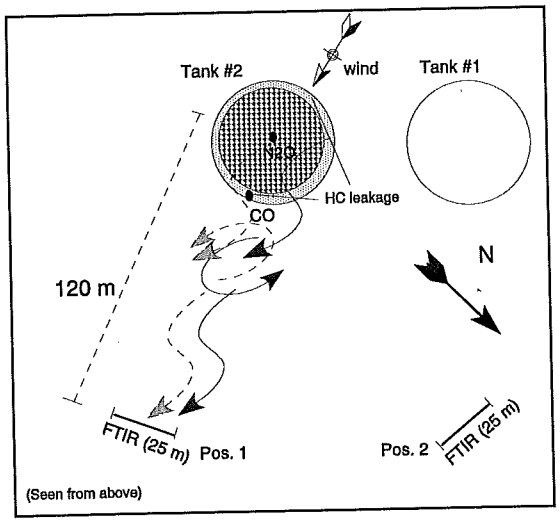

Figure 4.34 b) Schematic overview of the measurements in the tank park at the Scanraff refinery seen from above.

In Figure 4.35 and 4.36 results from a Gaussian simulation of the tanks in Figure 4.34 (a) and (b) are shown for two stability classes, neutral (D) and unstable (B). The plume width (95% of the mass) at ground level as a function of distance downwind is shown in Figure 4.35 while the mixing ratio profile at a distance of 100 downwind is shown in Figure 4.36.

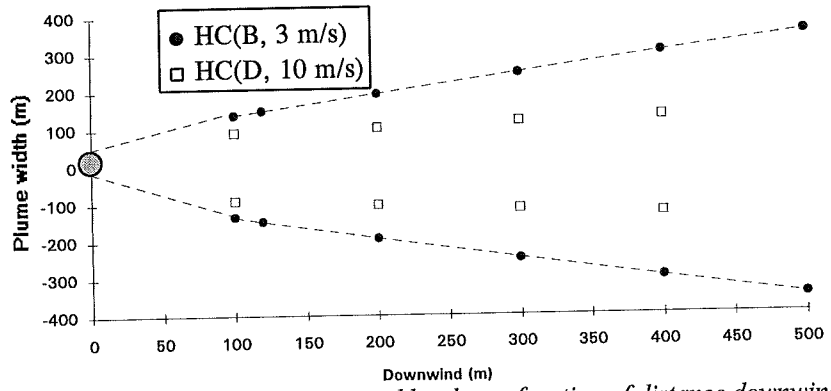

Figure 4.35. Plume width (95% of mass) at ground level as a function of distance downwind at two stability classes, neutral (B) and unstable (D).

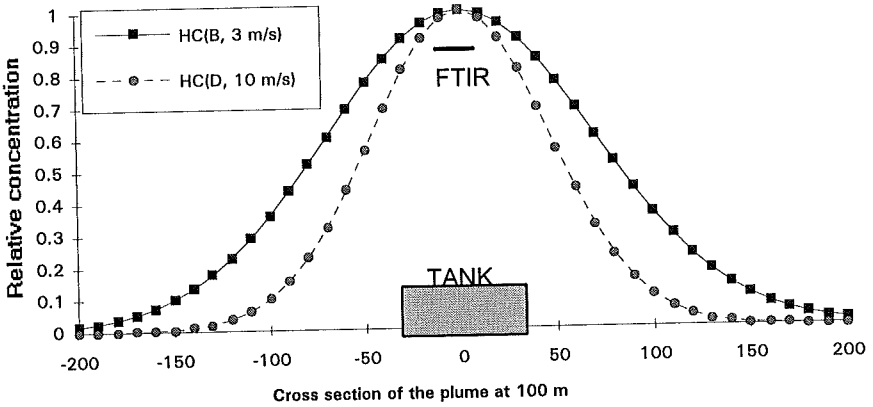

Figure 4.36. The concentrations over the cross section of the tank plume at a distance of 100 m downwind. Two stability classes were simulated neutral (B) and unstable (D).

4.6.1 Measurements

FTM measurements were performed in the beginning of August 1994. The winds were south westerly with moderate speeds (3-6 m/s). N_2O was used as a tracer with a leakage rate of 1 kg/h. The 1 km White system, Figure 2.2, was used at a distance of 120 m leeward of the tank.

In Figure 4.37 measurements are shown that were conducted at the Scanraff refinery on August 13, 1994. The figure shows the mixing ratios of the source gas (hydrocarbons in hexane equivalents) and tracer gas (N_2O) as a function of time at pos. 1. The roof level in the tank was 65% of its maximum level of 18 m.

In Figure 4.38 two absorbance spectra are shown in the CH stretch region. The fully drawn spectrum (*crude oil tank*) corresponds to the spectrum measured at 23:04 in the previous figure. Since the tracer mixing ratio was high here it can be deduced that the spectral features correspond to hydrocarbons emitted from the raw oil in tank no. 2.

The other spectrum, drawn with the dotted line (*undefined source*) was recorded at 22:42. It can be seen in Figure 4.37 that the tracer was very low here which implies that the spectral features then correspond to another undefined source. An analysis of the spectral features reveals that the crude oil spectrum is similar to hexane while the undefined source spectrum corresponds to a mixture of methane, ethane and propane. The crude oil spectrum in Figure 4.38 was used as a calibration spectrum. It was evaluated manually to 31.2 ppb hexane and 46.9 ppb of the hydrocarbon cocktail that was based on the Corinair (1994) data (as was previously discussed in section 3.1).

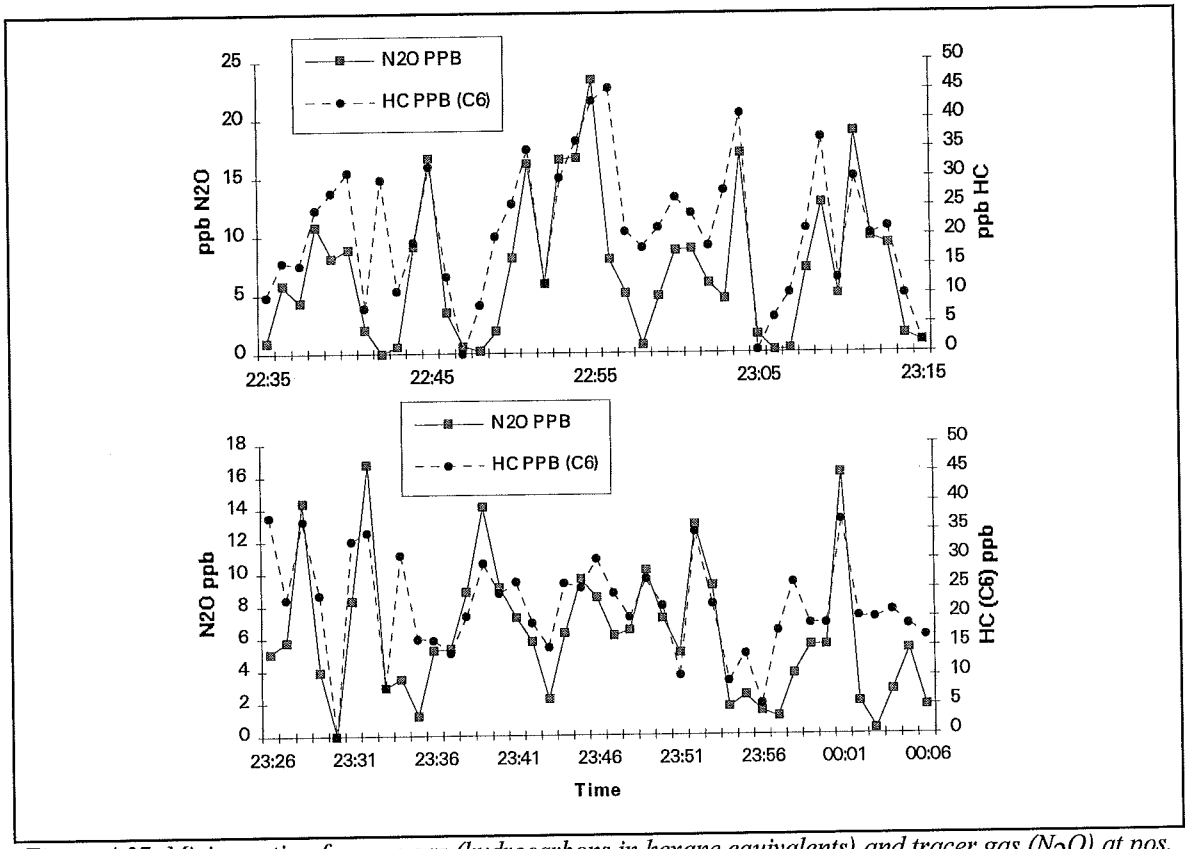

Figure 4.37. Mixing ratio of source gas (hydrocarbons in hexane equivalents) and tracer gas (N_2O) at pos. 1. The measurements were performed on August 13, 120 m downwind of tank 2.

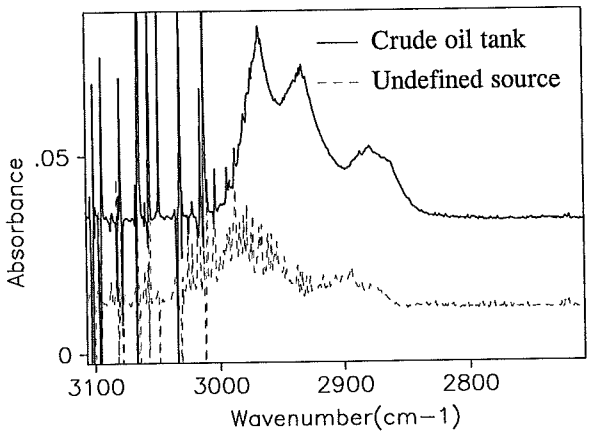

Figure 4.38. Absorbance spectra measured at position 1 on August 13, 1994. The spectrum shown with the full line corresponds to hydrocarbon emitted from the crude oil tank (no. 2). The other spectrum (dotted line) correspond to hydrocarbons from another (undefined) source at the refinery.

In Figure 4.39 a spectral fit is shown for which the calibration spectrum (obtained from the spectrum in Figure 4.38) was fitted to a spectrum that was measured at 23:31. The difference between the two spectra is also shown in Figure 4.39.
In Figure 4.40 a measured absorbance spectrum (*solid line*) is shown containing CO and N_2O. The spectrum corresponds to the spectrum measured at 22:38 in Figure 4.37. A synthetic calibration spectrum which has been simulated from HITRAN (Rothman et al., 1992) and then fitted to the measured one. In addition the difference between the measured and fitted spectra is shown.

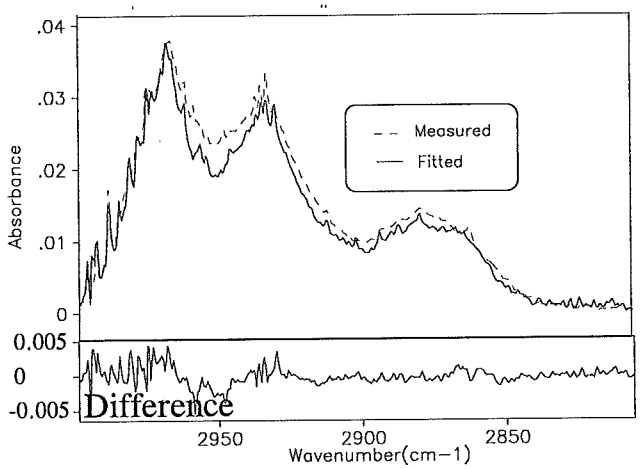

Figure 4.39. Typical fit in the CH stretch region and the difference between the two spectra is shown.

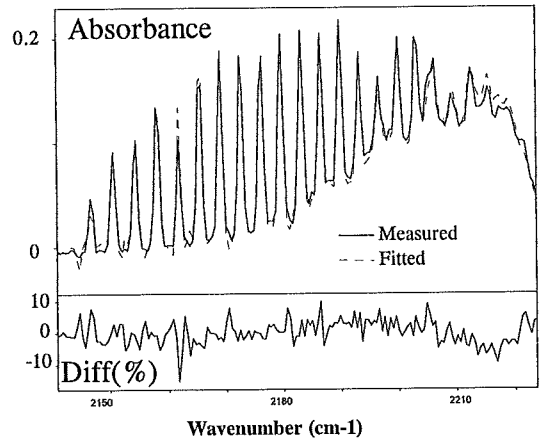

Figure 4.40. A measured absorbance spectra containing absorption features of the tracers CO and N_2O, and a fitted spectrum which was simulated from HITRAN. The sharp peaks correspond to CO while the broad structure correspond to N_2O. The relative difference between the two spectra is also shown.

In Figure 4.41 the tracer mixing ratio and the derived emission rates of hydrocarbons from tank no. 2 on the 13th of August are displayed. The data correspond to the ones shown in Figure 4.37. The tracer weighted average emissions are 4.6 kg/h and 5.5 kg/h, respectively (given in hexane equivalents). The standard deviations are 30% and 29%, respectively, indicating a reasonable source simulation by the tracer. The level of the tank was here 65% (of 18 m).

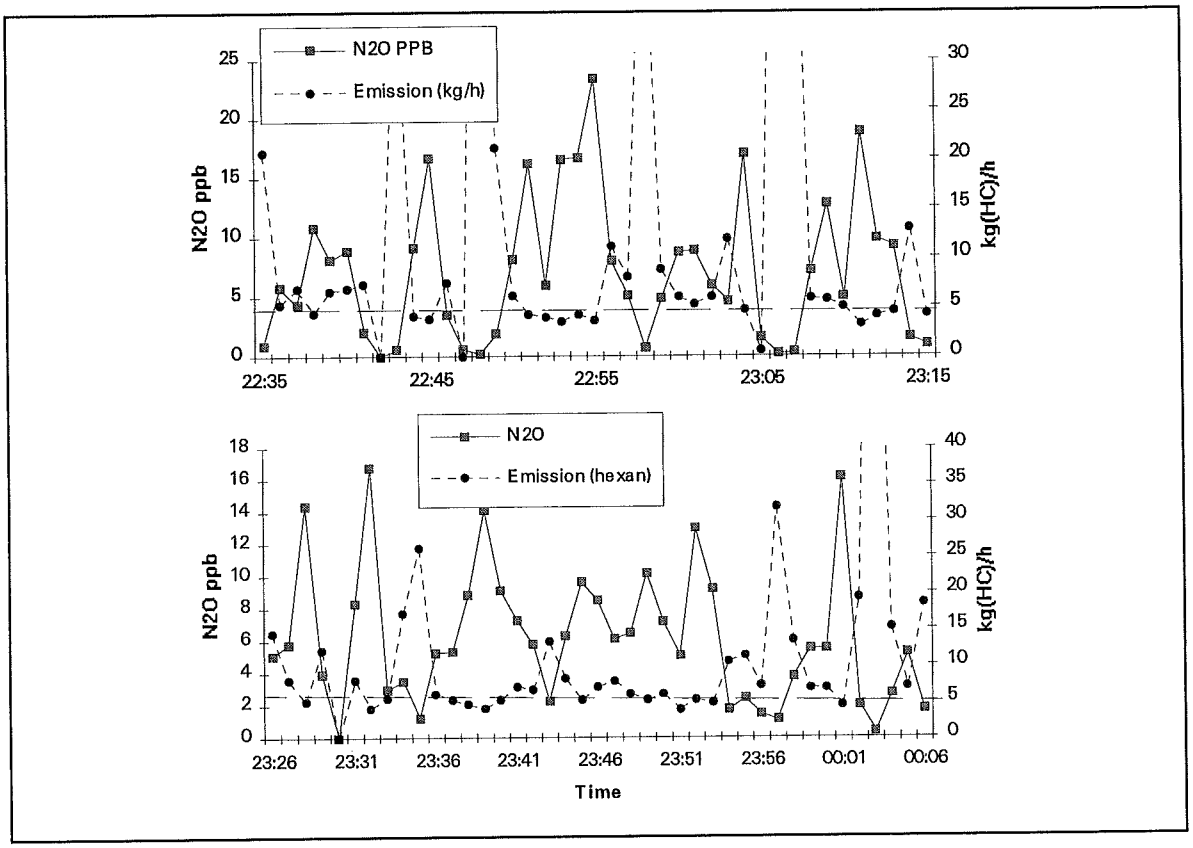

Figure 4.41. Mixing ratios of the tracer (N_2O) and derived leakage rates as a function of time.

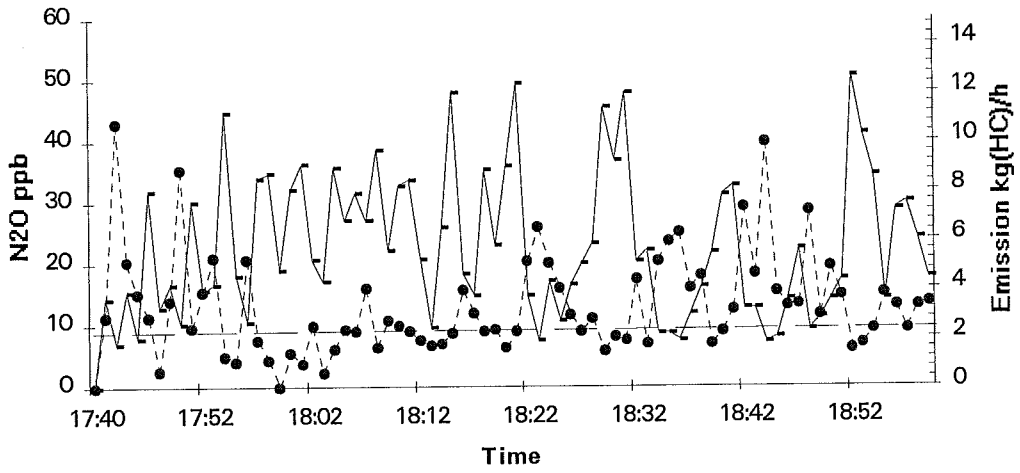

Figure 4.42. The mixing ratio of the tracer gas (N_2O) and derived leakage rate. Low wind speed, (< 3 m/s) gives large uncertainties in this measurement.

In Figure 4.42 results are shown from FTM measurement conducted on the same tank (no. 2) as in the previous figure but on the following day (August 14). The measurements were performed at pos. 2. Tank no. 2 was almost empty with a roof level of 15%. The winds were rather low, < 3 m/s, and therefore this measurement is associated with large uncertainties. The tracer weighted average is 2.3 kg/h with a standard deviation of 38%, which is rather high, thus reflecting the non-ideal meteorological conditions.

In Figure 4.43 the obtained leakage rates of tank no. 2 are shown together with the standard deviation of the emission rates, shown as error bars (±STD). The wind speed and tank level are also indicated.

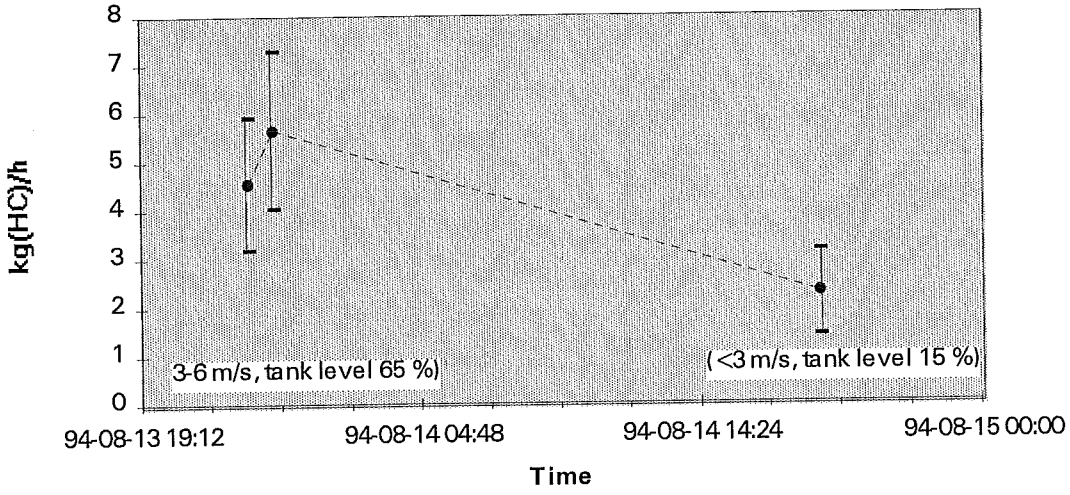

Figure 4.43. Derived HC emissions (hexane equivalents) from crude oil tank 2 at the Scanraff tank farm on August 1994. Each value corresponds to a weighted average over 30 data points. The weighted standard deviations in the emission rates are shown as error bars. Indicated are also the wind speed and tank level.

4.6.2 Experiment with different tracers.

Different tracers were used in order to evaluate the importance of the positioning of the tracer when conducting FTM measurements on oil tanks. In this study CO and N_2O were used with release rates of 4 and 1 kg/h, respectively. N_2O was emitted on top of the tank roof while CO was emitted on the leeward side of the tank, as illustrated in Figure 3.6 (a) and Figure 4.34 (a) and (b).

In Figure 4.44 (a) and (b) the mixing ratio of the two tracers are shown over time from 22:35 to midnight on August 13, corresponding to the same time period as in Figure 4.37. The measurement was performed at pos. 1 with wind speeds between 3 and 6 m/s. In Figure 4.44 (c) the derived emission rates of CO are shown, obtained by using N_2O as the tracer and then applying Eq. 14, as described in section 3.2. The weighted average of the CO emissions is 1.3 kg(CO)/h with a standard deviation of 50%. Since the real release rate of CO was 4 kg/h there is 68% error in the derived emission rate. This indicates that only a fraction of the emitted CO is getting mixed with the N_2O.

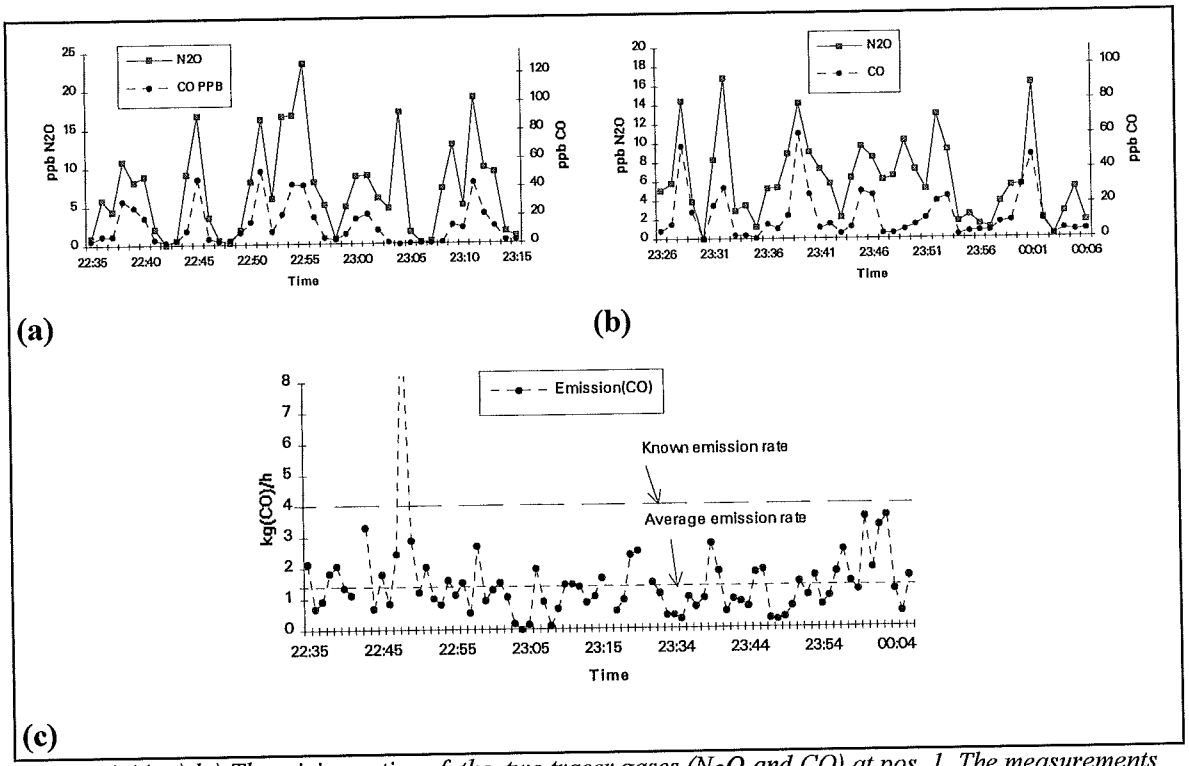

Figure 4.44. a) b) The mixing ratios of the two tracer gases (N_2O and CO) at pos. 1. The measurements were performed on August 13, 120 m downwind of tank 2. c) Derived emission rate of CO by using N_2O as the tracer. The real CO emission was 4 kg/h.

In Figure 4.45 (a) and (b) the mixing ratios of the tracers and the derived emission rates are shown for a measurement on August 14. The measurements were performed at pos. 2 with low wind speeds (< 3 m/s). The derived emission rate was here 2 kg(CO)/h with a standard deviation of 17%. Since the real release rate of CO was 4 kg/h, the error in the derived CO leakage rate corresponds to 50%.

In both Figure 4.46 (a) and (b) and 4.45 (a) it can be seen that time variations of the N_2O and CO mixing ratios are fairly similar. The time variation of N_2O however seem to

consist of two superimposed parts, of which one is identical to the time variation of the CO. The additional variations probably correspond to outbursts from the tank, which are caused by the wind blowing down into the tank. This explanation is further strengthened by the fact that many of these variations can be seen in the hydrocarbon mixing ratios which were measured at the same time, Figure 4.37.

To summarize the tracer experiments, these have shown that releasing the tracer leeward of the tank, compared to inside, will give large errors in the emission rates obtained from the FTM. These errors were probably caused by the fact that a smaller fraction of the CO than of the N_2O was transported into the wake, were the mixing of the two tracers occurred. It should be mentioned that the large errors obtained in this exercise are not anticipated in the hydrocarbon emissions that were derived by using N_2O as the tracer, since it was released inside the tank, at the level of the floating roof. The N_2O was only released in one point and in future work the use of several release points should be investigated.

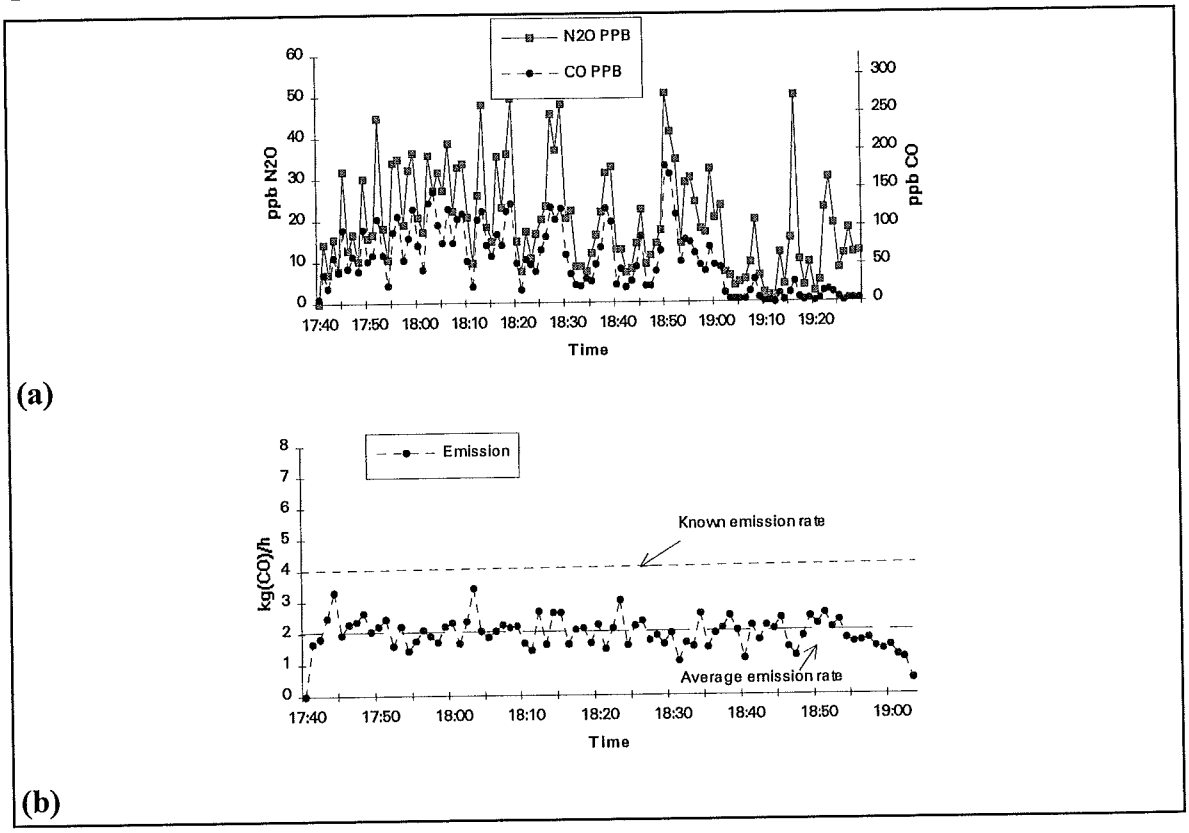

Figure 4.45. a) The mixing ratios of the two tracer gases (N_2O and CO) at pos. 2. The measurements were performed on August 14, 120 m downwind of tank 2. b) Derived emission rates of CO by using N_2O as the tracer. The true CO emission rate was 4 kg/h.

5. Results

In Table 4 the results from the FTM measurements are shown together with other results obtained with the conventional SF_6 method or with DIAL.
The results show a good agreement in obtained mass fluxes between the FTM and the conventional SF_6 method for measurements of alkenes. They also show that the instrumental concepts, as shown in Figure 2.2 and Figure 2.3, are quite versatile for this application. Except for developing and evaluating the FTM technique another aim in this study was to evaluate different optical configurations for mixing ratio measurements. In Table 5 a summary of some of the hardware parameters used for the measured species is shown including signal-to-noise and detection limits.

Table 4. Column 3 shows tracer weighted average emissions calculated over 0.5 to 3 h. The uncertainties correspond to the precision of several consecutive measurements (if available), based on 30 minute averages. In column 4 the tracer weighted standard deviations are shown. In column 5 the emission rates as measured by the conventional SF_6 (or DIAL) are shown. In column 6 the diffuse leakages that have been reported in the 1994 Environmental reports from each plant are shown. These values are either based on measurements or estimations.

Process area	Species	FTM kg/hr (±variability)	STD%	Other methods	Expected leakage rate 1994
Polyethylene high press.(95)	C_2H_4	28.8±16% (15/6) pos. 2	13-28		29
EO-plant (94) Reactor	C_2H_4	4.42±16% (24/8) pos. 2	10-25		< 13 (Total)
Cracker (95)	C_2H_4 C_2H_4 C_3H_6	13 (9/5) 15 ± 4% (12/5) 13.1 (12/5)	17 5-50 25	11.8±1.5 (9/5) 9 (9/5)	13.8 9.9
Cracker (93)	C_2H_4 C_2H_4	32 ±5% (1/4) pos. 3	8-17	29±5 (17/2) 25.5±2 (27/3)	29.9
Gas purific. Low press. 2 (94)	C_2H_4	3.1±16% (8/9)	19-56		5 process&gas purific.
Amine plant (94)	NH_3	1.1	28		< 1.2
Scanraff Crude oil tank (94)	C_2-C_6	5±10% (3/8-94) pos. 1 Tank level 65% 2.3 (4/8-94) pos. 2 Tank level 15%	30-38	5-265*	

* DIAL

Table 5. Hardware parameters for the FTM system used in this study. The pathlength for the single ended system (SE) is 200 m and 1 km for the White system. Water interference is not included.

Species	Wavelength region (cm^{-1})	Meas. system	Integrat. time (s)	Detector	Noise%	Detection limit (ppb)
Propane	2900-3100	White	60	InSb	0.05	0.5
Ethylene,	900-1000	SE(200) SE(200) White	10 60 60	MCT	0.1 0.05 0.3	3 1.5 1.5
Propylene	900-1000	White	60	MCT	0.3	1.8
NH3,	900-1000	White	60	MCT	0.3	2.1
CO	2150-2250	White	60	InSb	0.03	1.1**
N_2O	2150-2250	White	60	InSb	0.03	0.25**

6. Discussion

During the past year the FTIR Tracer Method (FTM) has been evaluated in a variety of field experiments in which the mass fluxes of several species have been quantified.

FTM measurements have been successfully conducted at 5 petrochemical process areas in Stenungsund. Most effort has been put into measuring ethylene, although measurements of both propylene and ammonia have been demonstrated as well. In the recorded spectra also other species could be retrieved, although this has not been of high priority in this study. For some of the measurements poor results were obtained. In these cases the wind speed was either too low and/or unstable or the measurements were performed too close to the source or the measurement were performed in the edge of the plume.

The FTM measurements were conducted on a range of sources with varying dimensions and leakage rates between 1 to 30 kg per hour. The distance from the source varied between 70 to 300 m.

The mixing ratio measurements were performed with long path FTIR technique. Two optical configurations were used. In the first (*the White system*) the light was transmitted 40 times between mirrors positioned 25 m apart, thus giving a total optical path length of 1 km. In the second configuration *(the single ended system*) the light was transmitted a distance of 100 to 200 m and then it is was reflected back to the detector by the use of a cube corner array. Good measurement results were obtained from both optical configurations. The second one was however easier to use, had less sensitivity to the wind and a larger light efficiency which made it possible to use a higher time resolution for this system.

A comparison between the conventional SF_6 method and the FTM indicates that the obtained leakage rates with the latter method are within the variability of the former method. The variability in the leakage rates obtained with the FTM were typically in the order of 15%. The reason for this variability could be either real variations in the emission rates or measurement artifacts.

There have only been a few mass flux measurements of alkanes from crude oil tanks. The results show that the FTM is a useful technique for alkane measurements from tanks although it is difficult to perform good tracer releases simulating the real leakages. In addition it is also more difficult to perform mixing ratio measurements of alkanes due to lower sensitivity of the available tracers and interfering absorption of water and other hydrocarbon species.

Future work

Compared to the conventional SF_6 method the FTM has the advantage that it can be automated and therefore used in a more continuous way than what is the case for the former method. It can therefore be used as a tool for determining variabilities in the emissions which is not possible with the conventional method. It is conceivable with an automatic FTM system where the tracer releases and mixing ratio measurements are performed automatically, triggered by meteorological conditions. In this study it has been demonstrated that in order to obtain a statistically significant emission value, it is sufficient with approx. 30 data points of the source and tracer concentration. It has also been shown that the Long Path measurement could be performed at a high time resolution (6 spectra/minute) and therefore a measurement period of only 5 minutes is

sufficient to obtain a reliable emission value. Under favorable conditions this could be repeated periodically over the day.
The general disadvantage with the FTM is that relatively inert tracer gases have to be released which all are climate gases. There are several ways to reduce this problem: First of all other less inert tracer gases can be used which dissociate fairly quick in the atmosphere and therefore give less environmental impact. Secondly the amount of tracer gas released can be reduced by performing measurements at a high time resolution as was previously mentioned. Finally if an automatic measurement system as described above could be implemented, it would be possible to develop an empirical dispersion model based on the tracer measurements and meteorological data of the wind, temperature and solar radiation. Such a model would thus be able to convert a measured mixing ratio to a mass flux for a given meteorological situation. Truly continuous mass flux measurements could thus be performed under favorable conditions with only a limited need for tracer releases.

The FTM has so far proven to be a usable and valuable tool for mass flux determination of fugitive emissions from both petrochemical process areas and crude oil tanks in oil refineries. For measurements of alkenes from process area the technique shows great promise and the obtained results have shown to be consistent with the results obtained from the conventional SF_6 method. In order to improve the technique the inherent uncertainties have to be studied further. First of all the uncertainties due to the tracer releases have to be understood, secondly uncertainties in the mixing ratio measurements should be further studied (detector nonlinearities, effects of interfering species). For measurements of alkane emissions from oil tanks more spectroscopic work needs to be conducted, in addition to field measurements and experiments with controlled tracer releases.

7. Acknowledgments

Financial support from Akzo Nobel Surface Chemistry AB, Borealis AB, the Swedish OK Environmental Research Foundation (OK miljöstiftelse) and the Swedish EPA (Naturvårdsverket) is gratefully acknowledged.

We would like to thank Jonny Andersson, Borealis, and Knut Andren, Akzo Nobel, for help and support in the project, as well as Dane Almfjärd, Per-Olof Eggöy and Ann Karlsson at the Borealis laboratory for performing the conventional SF_6 measurements and assisting with the tracer gas emissions.
We also would like to thank Urban Svedberg, YMK Sundsvall, for lending us an FTIR instrument and assisting during some of the measurements, Dag Tönnesen at the Norwegian Institute for Air Research (NILU) for assistance and discussions regarding the meteorology, David Griffith, University of Wollongong, for providing the SALT program.
In addition we also would like to thank many others for assistance during the measurements such as Anna-Lena Palm, Yngve Larsson, Leif Linder, Kenneth Johansson and K-G Mattson.

8. References

Andersson-Sköld, Y. Pleijel, K., "Miljörisker med Lösningsmedel-Vilket lösningsmedel ska jag välja". IVL report, B-1046, 1991.

Axelsson, H., McLaren, S., Galle, B., Mellqvist, J., Kloo, H. and Svedberg, U.,"Development of a Long Path Fourier Transform Infrared Instrument for Measurements of Diffuse VOC Emissions From the Automobile Industry", in proceeding of the international conference on Monitoring Toxic Chemicals and Biomarkers, Berlin 23-26 June, 1992.

Bojkov, R., J. of Clim. Appl. Met., 25, pp.345-352, 1986.

Corinair, "default emission factors handbook", ISSN 1018-5593, European Commission, Brussels, 1994.

Crutzen, P., "Ozone in the troposphere", to appear in Composition, Chemistry, and Climate of the Atmosphere (H., B., Singh, editor), Von Norstand Reinhold, Publ., October, **22**, 1993.

Galle, B., Klemedtsson, L. and Griffith, D.W.T.,"Application of Fourier Transform IR System for Measurements of N_2O Fluxes using Micrometerological Methods, an Ultra-Large Chamber System and Conventional Field Chambers", J. Geophys. Res., 99, (D8), 16569-16574, 1994.

Griffith, D.W.T., "Synthetic Calibration and Quantitative Analysis of Gas Phase FTIR Spectra.", accepted, J. of Appl. Spectrosc., 1995.

Griffiths, P.R. and deHaseth, J.A.,"Fourier Transform Infrared Spectrometry", John Wiley & Sons, New York, 1986.

Hanst, P.L. and Hanst, S.T.,"Gas Analysis Manual for Analytical Chemists", Infrared Analysis, Inc., Anaheim, California, 1990.

IPCC, Climate Change, The IPCC Scientific Assessment. WMO/UNEP., Houghton, J.P, Jenkins, G.J., and Ephraums, J.J., (Eds.), Cambridge University Press, Cambridge(UK).,1990.

Madronich, S. and Granier, C., "Impact of recent total ozone changes on on tropospheric ozone photodissociation, hydroxyl radicals, and methane trends", Geophys. Res. Lett., **19**, 37-40, 1992.

Mellqvist J, Galle, Bo,"Long-path-FTIR för Mätning av Diffusa Emissioner från Petrokemisk Industri", IVL-rapport B1122, Göteborg, februari, 1994.

Mellqvist, J.Arlander, B., and Kloo,H.,"Infraröd Fjärranalys för Mätning av Miljöstörande Gasformiga Ämnen i Verkstadsindustri", IVL-report ,B 1207, 1995.

Moldanova, J., "Oxidant formation in the Troposphere", ISSN 0283-8575, Licenciate thesis, Chalmers University of technology and Göteborg University, 1994.

Milton, M.J.T., Woods, P.T., et al.,"Applied Physics, B 54, 1992.

Pye, J. M, "Impact of ozone on the growth and yield of trees: A review", Journal of Environmental Quality **17**, 347-359, 1988.

Pleijel, H., Skärby, L., Wallin, G. & Selldén, G., "Yield and grain quality of spring wheat (Triticum aestivum L.,cv. Drabant) exposed to different mixing ratios of ozone in open-top chambers.", Environ. Pollut. **69**, 151-168., 1991.

Rothman, L.S., et al., "The HITRAN Molecular Database: Editions of 1991 and 1992", J. Quant. Spectrosc. Radiat. Transfer, **488**, 5/6, 469-507, 1992.

Sandnes, H., "Calculated Budgets for Airborne Acidifying Components in Europe, 1985, 1987, 1989, 1990 and 1991", EMEP/MSC-W Report 1/92, 1992.

Sivertsen, B., "Estimation of Diffuse Hydrocarbon Leakages from Petrochemical Factories", J. of Air. Poll. Cont. Assoc., 33(4), 1983.

Sommer, S.G., Mikkelsen, H., and Mellqqvist,J.,"Evaluation of meterological techniques for measurements of ammonnia loss from pig slurry", Agric. For. Meteorology, accepted., 1994

Staehlin, J., and Schmidt, Atmos. Environ. 25A, p.1739, 1991.

Wallin, G., "On the impact of tropospheric ozone on photosynthesis and stomatal conductance of Norway spruce, Picies abies (l.) Karst", dissertation, ISBN 91-86022-60-1,University of Gothenburg, Gothenburg 1990.

White, J.U.,"Long Optical Paths of Large Aperture", J. Opt. Soc. Am. 32, 285-288, 1942.

White, J.U.,"Very Long Optical Paths in Air", J. Opt. Soc. Am., 66,411, 1976.